

GENERATION OF AN H3N2 INFLUENZA A REPORTER VIRUS TO VISUALIZE MODERN INFECTION DYNAMICS

by

Emily Thompson

A thesis submitted to Johns Hopkins University in conformity with the
requirements for the degree of Master of Science

Baltimore, Maryland

April 2018

ABSTRACT

The public health burden of influenza is exacerbated by the continuous emergence of new strains and unanswered questions about viral spread within the host. Previously, groups have utilized reporter viruses encoding fluorescent proteins or luciferases to visualize real-time infection dynamics and elucidate complex interactions between viruses and host cells. In 2013, Tran et. al. developed a replication-competent influenza A reporter virus expressing nanoluciferase in the PA segment of a 1933 strain of H1N1, A/WSN/33, that closely mimicked wild-type virus behavior and replication dynamics. However, currently circulating strains of influenza are predominantly H3N2 viruses, urging development of a reporter influenza A virus that more closely represents the behavior of these modern strains. To address this need, we aimed to create two influenza A reporter viruses expressing nanoluciferase and the fluorescent protein mPlum in the PA segment of the A/Victoria/361/2011 strain of H3N2. Through various cloning techniques, the reporter genes were inserted at the end of the PA segment, and a reverse genetics approach was used to generate the two reporter viruses. Characterization of infectious titers and replication kinetics of the reporter viruses in cell culture (through TCID₅₀ and plaque assays) demonstrated that the mPlum reporter virus, rA/Vic-mPlum, was slightly attenuated compared to the nanoluciferase reporter virus, rA/Vic-NLuc, and the wild-type virus, rA/Vic-WT. In addition, expression of mPlum fluorescent protein in the reporter virus could not be validated. However, rA/Vic-NLuc stably maintained luciferase activity and grew to higher titers and with similar kinetics as rA/Vic-WT. The results suggest rA/Vic-NLuc is replication competent and can be used in future applications to quickly

assess the behavior of emerging H3N2 influenza viruses and further investigate influenza A virus replication and pathogenesis.

ACKNOWLEDGEMENTS

I would like to express my deepest gratitude to my thesis advisor, Dr. Andrew Pekosz. His ceaseless guidance and passion for virology not only made this thesis possible, but also inspired me to pursue a career that advocates translation of laboratory science into real-world solutions. I also owe a great thank you to Dr. Farah El Najjar, who taught me everything from fluorescent microscopy and virus titering to cell culture and reverse genetics. I am extremely grateful for her continuous patience and mentorship.

Thank you to all other members of the Pekosz laboratory, past and present – Laura Canaday, Dr. Katherine Fenstermacher, David Jacobs, Dr. Hsuan Liu, Harrison Powell, Dr. Katy Shaw-Saliba, Brendan Smith, Robert Stenzel, and Dr. Nick Wolgemuth – for sharing the everyday laboratory experience with me and providing kind encouragement over the last two years. I would also like to thank Dr. Sabra Klein for her thoughtful feedback and suggestions over the course of my thesis research, and Dr. Kim Davis for her recommendations on troubleshooting fluorescent imaging and helpful comments during lab meetings.

A special thank you to my fiancé, Kevin Chavez, who encouraged me to pursue my graduate degree and whose unwavering love and support helped me succeed. Thank you also to my parents, Russ and Lori Thompson, who taught me to love learning and always stay curious. Lastly, thank you to my brother, Jack, for reminding me how grateful I am to study biology and not engineering physics.

CONTENTS

CHAPTER 1: INTRODUCTION.....	1
1.1 Influenza.....	1
Overview.....	1
Epidemiology.....	1
Public Health Concern	2
1.2 Influenza Genome and Diversity.....	2
Virion Structure	2
Antigenic Drift – HA	3
Antigenic Drift – NA	4
1.3 Pandemic Influenza.....	5
Animal Reservoirs	5
Public Health Impact.....	5
Antigenic Shift.....	6
1.4 Issues with Influenza Control.....	7
Challenges.....	7
1.5 Influenza Replication	9
Overview.....	9
Replication of Genomic vRNAs and Transcription of mRNAs	10
1.6 Reporter Viruses.....	11
Introduction.....	11
Influenza A Reporter Virus Challenges and Applications.....	12

1.7 Project Overview	14
CHAPTER 2: REPORTER CONSTRUCT CLONING AND EXPRESSION	15
2.1 Background	15
Selection of Reporter Genes	15
Use of Mammalian Expression Vector	16
2.2 Methods	17
Generation of PA-Reporter Constructs	17
Gibson Assembly	19
Site-Directed Mutagenesis	21
Bacterial Colony Screening and Sequence Analysis	23
Expression Validation	24
Cell Lines	24
Nano-Glo [®] Luciferase Assay for NLuc in pCAGGS-PA-NLuc	24
Western Blot for PA in pCAGGS-PA-NLuc	25
Fluorescence Microscopy of mPlum in pCAGGS-PA-mPlum	27
2.3 Results	28
Nano-Glo [®] Luciferase Assay	28
Western Blot	28
Fluorescence Microscopy	29
Conclusions	29
CHAPTER 3: REPORTER VIRUS CHARACTERIZATION	31
3.1 Introduction	31

Background	31
Reverse Genetics Approach	31
Virus Characterization	32
3.3 Methods	33
Sub-cloning of PA-reporter Gene Constructs into pHH21	33
Reverse Genetics and Virus Rescue	34
Virus Plaque Assay and Clone Isolation	35
Viral RNA Isolation	36
TCID ₅₀ Assay	37
Plaque Morphology	37
Nano-Glo [®] Luciferase Assay	38
Immunofluorescence of rA/Vic-mPlum	38
Low MOI Growth Curve	40
Graphing and Statistical Analysis	40
3.4 Results	42
Virus Rescue	42
Titers of Generated Recombinant Viruses	42
Nano-Glo [®] Luciferase Assay	43
Immunofluorescence of rA/Vic-mPlum	44
Low MOI Growth Curve	44
CHAPTER 4: DISCUSSION	46
4.1 Overview	46

4.2 rA/Vic-mPlum	46
4.3 rA/Vic-NLuc	48
4.4 Future Directions.....	49
<i>Overview</i>	49
<i>Live-Cell Imaging</i>	50
<i>Seasonal Influenza Transmission Dynamics</i>	50
<i>Serum Antibody Neutralization Alternative</i>	51
REFERENCES.....	74
Appendix	74
Bibliography.....	76
Curriculum Vitae.....	84

LIST OF TABLES & FIGURES

TABLES	
Table 1: Primer Sequences	57
Table 2: Sequencing Primers Only	58
FIGURES	
Figure 1: Influenza virus structure	53
Figure 2: Structure of the influenza A polymerase complex	53
Figure 3: PA-SWAP-2A-NLuc50 (PASTN) construct by Tran et. al.....	54
Figure 4: Project outline.....	54
Figure 5: Restriction enzyme digestion of pCAGGS-mPlum.....	55
Figure 6: Overlap extension PCR for addition of PA50 to mPlum.....	55
Figure 7: Restriction enzyme digestion for the generation of linearized pCAGGS.....	56
Figure 8: Sequence alignment show a frameshift mutation in pCAGGS-PA-mPlum ...	59
Figure 9: Sequences of PA segments of H3N2 strains shows conservation of W422 ...	59
Figure 10: Validation of nanoluciferase expression in pCAGGS-PA-NLuc	60
Figure 11: Validation of PA protein expression in pCAGGS-PA-NLuc	61
Figure 12: Fluorescence microscopy of mPlum expression in pCAGGS-PA-mPlum...	62
Figure 13: Addition of BsaI restriction sites to PA-mPlum and PA-NLuc by PCR	63
Figure 14: Restriction enzyme digestion of PA-mPlum, PA-NLuc, and pHH21	63
Figure 15: Schematic of the reverse genetics process for creating influenza viruses	64
Figure 16: Sequencing results of the working stock of rA/Vic-WT	65
Figure 17: Sequencing results of the working stock of rA/Vic-NLuc	65

Figure 18: Sequencing results of the working stock of rA/Vic-mPlum	66
Figure 19: Working stock titers of rA/Vic viruses by TCID ₅₀ and plaque assay	67
Figure 20: Plaque assay of MDCK cells infected with WT and reporter viruses	68
Figure 21: Comparison of plaque areas formed by WT and reporter viruses	69
Figure 22: Luciferase Activity of the rA/Vic-NLuc reporter virus	70
Figure 23: Fluorescence microscopy for evaluation of the rA/Vic-mPlum	71
Figure 24: Replication kinetics of WT and reporter viruses	72

CHAPTER 1: INTRODUCTION

1.1 – INFLUENZA

Overview

Influenza is a respiratory disease that infects respiratory epithelial cells and causes mild to severe illness in humans. Symptoms of influenza infection include a rapid onset of fever, headache, cough, sore throat, runny or stuffy nose, myalgia, and fatigue.¹ While influenza infection typically presents as an acute febrile respiratory tract infection, damage to the epithelial cell barrier can lead to systemic responses and increased susceptibility to secondary bacterial infections including pneumonia.² Influenza disease in humans can be caused by Influenza A, B, or C viruses, however, infection with Influenza C virus causes very mild disease, while Influenza A and B viruses cause seasonal epidemics that result in moderate to severe morbidity globally.³ This thesis focuses on Influenza A virus (IAV).

Epidemiology

IAV is transmitted through respiratory droplets and aerosols that can travel up to six feet when an infected individual coughs, sneezes, or talks.⁴ In addition, IAV can be spread through contact with fomites, which can harbor infectious influenza virus particles for up to 8 hours.⁵ When a susceptible individual inhales respiratory droplets containing the virus, IAV attaches and infects epithelial cells of the upper respiratory tract.⁶ On average, the incubation period of IAV is 1.4 days before an individual develops symptoms, however infected hosts can transmit the virus to others before symptoms

develop. In addition, the average R_0 value of seasonal Influenza A is 1.75, meaning that in a fully susceptible population a single infectious individual will transmit the virus to 1.75 other individuals.⁷

Public Health Concern

While influenza is typically regarded as a mild illness, IAV infects 5-15% of the global population⁸ and causes hundreds of thousands of hospitalizations every year⁹. In the US alone, influenza causes 24,000 deaths annually, while the global count ranges between 250,000-500,000 deaths per year¹⁰. The populations that are at the highest risk of developing severe disease from influenza infection are young children and the elderly in addition to immunocompromised individuals and pregnant women.

1.2 – INFLUENZA GENOME & SOURCES OF DIVERSITY

Virion structure

Viral protein functions will be discussed in more detail later in this chapter, but a brief introduction is needed in order to discuss the clinical and public health significance of influenza. Influenza A virus is a negative single-stranded RNA virus and is part of the *Orthomyxoviridae* family (**Figure 1**). Its genome is comprised of 8 individual segments that replicate as autonomous units within an infected cell.¹¹ On the surface of the influenza virus particle are the glycoproteins hemagglutinin (HA) and neuraminidase (NA). HA allows the virus to bind to receptors that contain sialic acid residues and infect cells, while NA facilitates the release of newly formed virus particles from an infected

cell.¹² In addition to these surface proteins, the matrix 2 protein (M2) sits within the viral lipid bilayer and plays a critical role in viral entry, uncoating, autophagy inhibition, and the production of infectious influenza virus particles.¹³ In comparison, the inner surface envelope matrix 1 protein (M1) functions during virion assembly and budding.

The core of the influenza virus contains the viral RNA segments that encode these proteins in addition to several others. The PB1, PB2, PA segments that form the influenza RNA-dependent RNA polymerase complex and the influenza nucleoprotein (NP) that protect the viral genome during replication are also contained in the core of the virion.¹⁴ The nuclear export protein (NEP or NS2) plays an important role in shepherding the viral gene segments from the nucleus to sites of virus particle budding. Lastly, the non-structural protein, NS1, encoded in the NS segment, has a variety of roles including host antiviral gene expression inhibition, but is not packaged into virus particles at an appreciable amount.¹⁵

Antigenic Drift – HA

Influenza is continuously evolving and pushing the boundaries of the global public health response. One of the reasons for this rapid evolution is influenza has a genome made of RNA, and RNA polymerases lack the proofreading mechanism present in DNA polymerases.¹⁶ Therefore, any errors or mutations made during the replication of the influenza genome are maintained. In cases where these mutations are beneficial to viral fitness, the virus survives in the population and outcompetes weaker influenza viruses. Most often, the adaptations that accumulate in circulating influenza strains

involve changes to the surface glycoprotein HA. Changes to the HA sequence can allow the virus to avoid detection by host antibodies and "drift" away from current vaccine formulations.¹⁷ This process of *antigenic drift* dictates the need to reevaluate the strains included in the influenza vaccine every year to assure protection against current HA surface antigens.

Antigenic Drift – NA

While NA antigenic drift occurs less frequently than HA drift, NA plays a key role in mediating protection from influenza. The enzymatic activity of NA is essential for the release of virus particles from an infected cell and allows IAV to be transmitted in small droplets.¹⁸ Previous studies demonstrated an association between high anti-NA antibody titers and less severe symptoms and lower levels of viral shedding.¹⁹ More recently, data show that anti-NA antibodies can protect mice from lethal challenge with IAV, and anti-NA antibodies bind with remarkably broad specificity unlike their HA counterparts.²⁰ Despite these data, current influenza vaccine production does not standardize quantification of the NA component in vaccines, nor do current vaccines induce NA-reactive B cells.²¹ Further attention should be paid to the NA component of influenza vaccines to increase efficacy and address seasonal antigenic drift.

1.3 – PANDEMIC INFLUENZA

Animal Reservoirs

Migratory waterfowl are the primary reservoir of influenza A viruses including all 16 subtypes of hemagglutinin and 9 subtypes of neuraminidase.²² In these species, influenza infection usually presents as a minor gastrointestinal disease rather than an infection of the respiratory tract, and influenza viruses infect the epithelial cells of the intestines that express primarily $\alpha 2,3$ - sialic acid linkages. Comparatively, human respiratory epithelial cells contain sialic acids linked to the penultimate galactose through mainly $\alpha 2,6$ - linkages.²³ Domesticated poultry can also serve as animal reservoirs for influenza viruses and HA subtypes H5, H7, and H9 circulate naturally in these populations. In addition to avian species, swine carry influenza virus strains that circulate exclusively in that species. Influenza A viruses that circulate in swine have already overcome a number of species barriers that prevent avian influenza viruses from efficiently infecting mammals. Swine may also serve as intermediate hosts, or “mixing vessels” for influenza viruses from different species (avian, human, etc.). The epithelial cells in the respiratory tract of pigs contain high amounts of both Sia $\alpha 2,3$ Gal and Sia $\alpha 2,6$ Gal sialic acid linkages and can therefore be infected by influenza viruses arising from both avian and human sources.

Public Health Impact

In six months, the Great Influenza pandemic of 1918 infected one-third of the entire global population and killed more than 50 million people.²⁴ Responsible for more

than the casualties of both World War I and II combined, the 1918 influenza defined many of the infectious disease control measures still practiced today. The genome of the virus that was responsible for the pandemic in 1918 contained all 8 segments from avian species and was completely novel to humans in all aspects. In 1957, the Asian Flu emerged as a reassortant of the 1918 H1N1 virus and an H2N2 virus. Another avian human influenza virus reassortment led to the H3N2 influenza pandemic of 1968. Most recently, in 2009, the “Swine Flu” H1N1 pandemic emerged as a triple reassortant virus containing original segments from avian, human, and swine influenza viruses and appears to have been a result of a direct swine to human transmission event.²⁵

Antigenic Shift

The segmented genome of IAV allows it to reassort with other IAV strains to generate viruses with new gene segment combinations very easily. When a single cell is infected with two or more influenza virus strains, the eight segments of the genome can shuffle together, generating a new virus particle that contains a mix of segments from either of the two original viruses.¹¹ For example, if a single cell is infected with two different influenza viruses, there are 254 potential variants can emerge as a result of the co-infection event. While this process of reassortment allows influenza to regulate viral fitness to maintain circulation and survival within a population, a possible combination of avian sequences and human sequences packaged into the same virus can lead to a pandemic.

Humans have been exposed to influenza HA types 1, 2, and 3 naturally over the course of evolution, however, there is no pre-existing immunity against the other HA subtypes in the broader human population. As a result, when viruses of the other HA subtypes from animals cross the species barrier into humans, a pandemic can emerge if there is sustained human-to-human transmission of the new virus. This phenomenon is referred to as *antigenic shift* and is the reason behind the pandemics of 1918, 1957, 1968, and 2009. For a virus to cross the species barrier from either avian or swine species into humans, the influenza virus must be able to 1) attach to the surface of human cells 2) replicate its RNA inside human cells 3) inhibit aspects of the immune response to infection and 4) overcome the temperature barrier to be able to replicate at lower temperatures.²⁶

1.4 – ISSUES WITH INFLUENZA CONTROL

Challenges

Influenza continues to challenge modern public health systems due to its unique genetic structure and widespread global presence. First, the virus causes yearly epidemics that arise from unpredictable antigenic drift. As an RNA virus, influenza lacks the proofreading mechanisms involved in viral transcription that are present in both DNA viruses and human DNA. When minor errors in transcription occur, there is no repair mechanism to fix the mutations and either the conferred mutations hurt the virus and it dies out in the population, or the mutations improve viral fitness and the virus can sustain

itself well in the population. Moreover, these rapid changes in viral RNA can lead to antiviral drug resistance.²⁷

Another challenge with influenza control is the inefficient and timely process of vaccine development. Influenza vaccines are grown in embryonated hen's eggs where each infected egg generates 1-3 vaccine doses.²⁸ To make the vaccine, the HA and NA surface glycoproteins from circulating or emerging flu strains are mixed with internal genes of a well-characterized vaccine virus that is adapted for growth in eggs. However, if the selected HA and NA genes result in a virus that cannot grow well in eggs, the virus can no longer be used as the vaccine due to manufacturing limitations.²⁹ Vaccine strains are typically chosen in March of every year based off circulating viruses from the previous year. Yet, in March, the flu season is still not fully over, and selected vaccine viruses may miss emerging strains that arise at the end of the flu season. For example, in 2003, an A/Fujian H3N2 virus emerged in the month of March, but the number of isolates was small compared to the A/Panama/2007/99 vaccine strain isolates. Moreover, attempts to try to grow the A/Fujian strain in eggs failed.³⁰ Because there are no approved alternate technologies for influenza vaccine production and because the number of isolates of A/Fujian were limited, the virus was not included in the final vaccine selection for the 2003-2004 season. Consequently, manufacturers maintained the A/Panama strain in the vaccine and the cases of H3N2 that emerged in the 2003-2004 season were all A/Fujian strains, resulting in very low vaccine efficacy.³¹ Cases like the vaccine mismatch in 2003 serve as a reminder of the inefficient and costly production of influenza vaccines and are currently driving the initiative to create a "universal" influenza

vaccine that can target more conserved regions of the virus to induce protection for multiple years at a time.

1.5 – INFLUENZA REPLICATION

Overview

The replication of influenza viruses is a complex process that is carried out by genes encoded on multiple segments of the influenza genome and takes place within the nucleus of an infected cell. Inside the nucleus, the virus can avoid detection by antiviral responses common in the host cytoplasm. In addition, the nucleus of the cell contains the highest concentration of host messenger RNA as well as splicing machinery that can be hijacked by the influenza virus. Together, the polymerase acidic protein (PA) and polymerase basic proteins 1 and 2 (PB1, PB2) form a heterotrimer that functions as the RNA-dependent RNA polymerase (RdRp), **Figure 2**. NP is also involved in viral replication, and encapsidates the viral genome to form the ribonucleoprotein (RNP) that protects RNA during transcription and packaging.³² Upon viral entry into the host cell, a low pH pulse mediated by the M2 protein frees the RNPs from the M1 protein. This process unmask nuclear localization signals (NLSs) contained in the NP core of the RNPs and facilitates the active transport into the host nucleus.^{33,34} Normally, proteins only 40-50 kDa in size can passively enter through nuclear pores, while these RNPs can be upwards of 2500 kDa and require the help of host nuclear import mechanisms.

Replication of Genomic vRNAs and Transcription of mRNAs

The influenza RdRp is used to both replicate viral genomic RNA and to generate mRNA for the translation of viral proteins. Once inside the nucleus, the viral genomic RNA (vRNA) is both replicated through complementary RNA (cRNA) intermediates and transcribed into mRNA for the production of viral proteins.^{35,36} Recent studies suggest the interaction between PA and the minichromosome maintenance (MCM) complex allows stabilization of the polymerase complex that supports the full elongation of vRNAs during the synthesis of cRNAs.³⁷ However, the exact role that the PA segment plays in this replication of vRNA is not well characterized.³⁸

To generate mRNA, the PB2 segment of the RdRp facilitates the “cap-snatching” phenomenon by binding to the 5’ methylated caps of host cell mRNA and stealing these sequences as primers for generation of its own viral RNA. The 5’ caps are then cleaved by an endonuclease encoded in the PA subunit of the RdRp and are used by PB1 as primers for the transcription of viral mRNAs.³⁹ Eventually the 5’ end of the viral genomic RNA is still bound by PB1 and the polymerase lacks the strength to pull this 5’ end away, leaving approximately 20 nucleotides stuck in the RdRp complex. This sequence is preceded by a stretch of uridines, and as the viral polymerase engages in a tug-of-war with the RNA, the polymerase stutters across this uridine-rich region, generating a string of adenosine nucleotides on the end of the mRNA that serve as the poly-A tail required for replication.⁴⁰ These newly generated positive-sense mRNAs can then be exported to the cytoplasm for the translation of viral proteins,⁴¹ which are trafficked to the plasma membrane and assembled into complete virions. Finally, NA

mediates cleavage of HA from sialic-acids on the host cell and allows detachment and maturation of the influenza virion.

REPORTER VIRUSES

Introduction

Viruses that are engineered to express virus-inducible reporter genes with fluorescent or enzymatic activity are termed *reporter viruses*. The concept of using fluorescent proteins to study molecular interactions between a host and pathogen is incredibly useful and has a large range of potential applications. For example, in 2011 researchers engineered dengue reporter viruses of serotypes 1-4 that expressed green fluorescent protein (GFP). These reporter viruses were used to quickly determine neutralizing antibody titers from human serum samples, and suggest an alternate approach of quantification besides traditionally used plaque reduction neutralization tests (PRNT).⁴² Other groups have also used dengue reporter viruses to visualize viral replication concentrated in the lymphoid and gut-associated tissues of mice, and were successful in demonstrating how this localization changes over time.⁴³ Besides dengue reporter viruses, in 2014, the Freeman et al. group used a murine hepatitis reporter virus to elucidate the targeting and activity of replicase proteins during infection.⁴⁴ Measles is also another virus that has been engineered frequently as reporter viruses to study pathogenesis and cellular interactions; in 2016 Singh et al. created a GFP-labeled measles virus in order to observe the cell-to-cell transmission of the virus *in vitro*.⁴⁵ These are just

a few examples of how reporter viruses are useful for both *in vitro* and *in vivo* exploration of virus-host interactions.

Influenza A Reporter Viruses, Challenges, and Applications

Similar to the applications discussed above, influenza A reporter viruses have been used to explore neutralizing antibody screening techniques, antiviral compound efficiency, cell tropism, critical host factors, and vaccine development possibilities.⁴⁶ However, IAV presents unique challenges to scientists attempting to construct influenza A reporter viruses. First, influenza poorly tolerates gene insertions. Second, viral replication of reporter viruses is often attenuated *in vitro*, *in vivo*, or both. Finally, inserting fluorescent genes at the ends of influenza gene coding regions can disrupt packaging signals that are required for assembly of the virus particle. These challenges are demonstrated more in depth with examples of previous work generating influenza A reporter viruses.

The first attempts to generate influenza reporter viruses were made in 2004 by groups at the Institute of Applied Microbiology in Vienna, Austria and the Institute of Medical Science at the University of Tokyo. Both attempts involved replacing regions of the NA or NS1 segments with GFP, and the groups demonstrated reporter virus attenuation⁴⁷ and decreased pathogenesis in mice.⁴⁸ Other research groups tested Gaussia luciferase insertion, rather than GFP, into the PB2 and NA segments of A/PR/8/34. While these reporter viruses demonstrated strong fluorescence *in vivo*, there was significant reporter virus attenuation *in vitro*.⁴⁹ Later, in 2010, Manicassamy et al. introduced

reporter genes, including luciferases, into the NS segment of a 1934 H1N1 strain from Puerto Rico (A/PR/8/34). However, their attempts either resulted in background levels that were too high for detection, reporter virus attenuation, or loss of reporter expression after passaging in cells.⁵⁰ In order to increase the stability and pathogenicity of the Manicassamy et al. generated influenza reporter viruses, Fukuyama et al. serially passaged the reporter virus in mice.⁵¹ While this did slightly improve pathogenicity and stability of the reporter virus, their experiments used the NS reporter gene construct from the A/PR/8/34 H1N1 strain in the context of an H5N1 backbone. Therefore, any conclusion drawn from the behavior of this reporter virus may not accurately depict behavior of the wild-type virus. Moreover, the group identified two mouse-adapted mutations in the HA and PB2 segments of the reporter virus following passage.

In 2013, a group led by Andrew Mehle at the University of Wisconsin Madison constructed a relatively stable influenza reporter virus using the PA segment from a 1933 strain of H1N1 (WSN) with nanoluciferase as the reporter gene.⁵² The construct design that demonstrated the lowest levels of reporter virus attenuation is shown in **Figure 3**. In this design, the PA packaging sequence was moved to the end of the segment following the nanoluciferase gene, in order to avoid disrupting the critical role this sequence has in packaging the segment into a complete virion. The group also included silent mutations where the packaging sequence used to be to ensure any direct repeats were removed and transcription would proceed with the nanoluciferase gene. Lastly, the construct by Tran et al. included a 2A self-cleaving peptide from a picornavirus to allow cleavage of the reporter gene from the PA segment.

Project Overview

Reporter viruses are invaluable for visualizing real-time infection dynamics and may help elucidate complex interactions between viruses and host cells. In this project (**Figure 4**), a fluorescent protein, mPlum (far-red), and a nanoluciferase reporter, NLuc, will be inserted into the PA segment of the A/Victoria/361/11 (A/Vic) H3N2 influenza virus isolated in 2011. Packaging signals of the PA segment will be moved to the end of the construct to allow complete expression of the reporter genes. Silent mutations will also be inserted into the PA gene to optimize for expression in human cells. The PA-reporter gene construct will then be utilized in a reverse genetics approach to create reporter viruses. Following successful generation of the PA reporter virus, comparative infection studies will help determine any effects of the inserted reporter genes on virus replication compared to the wild-type virus. Later, the reporter construct can be used in visualization experiments to analyze real-time infection of influenza viruses.

CHAPTER 2: REPORTER CONSTRUCT CLONING & EXPRESSION

2.1 – BACKGROUND

Selection of Reporter Genes

The reporter viruses that were generated as part of this project incorporated the genes encoding either the fluorescent protein mPlum or the small enzyme nanoluciferase (NLuc). These reporter genes were selected for their range of potential application *in vitro* and *in vivo*.

mPlum is a 681-base pair far-red monomeric protein that emits light when exposed to wavelengths around 649 nanometers (nm). As the deepest colored fluorescent protein in the far-red spectrum, which ranges from 630-700nm, mPlum is useful for imaging specimens that may otherwise have naturally high levels of green autofluorescence.⁵³ In addition to this preferred low signal to noise ratio, expression of mPlum can be detected directly when imaging within the Cy5 channel, and therefore does not require addition of a substrate to induce fluorescence. These characteristics make mPlum particularly useful in live animal imaging when a substrate cannot be given systemically and there is a need to minimize autofluorescence. Moreover, mPlum has excellent photostability and can be used in multicolor imaging applications with fluorescent proteins emitting at lower wavelengths.⁵⁴ However, despite these benefits, the far-red fluorescent proteins are known for lower than desired brightness, which may make detection more challenging.⁵⁵

The other reporter protein selected for generating an influenza A reporter virus is nanoluciferase (NLuc), which was used previously by Tran et al.⁵² NLuc is a genetically modified luciferase that is expressed naturally in a deep-sea shrimp and is much smaller and brighter than traditional luciferases. NLuc is only 513-base pairs and 19 kDa compared to Renilla, and Firefly luciferases at 36 and 61 kDa respectively. NLuc is also approximately 100-fold brighter than either of these more commonly used luciferases.⁵⁶ As a result of its small size, NLuc is able to penetrate thicker tissues *in vivo*. Similar to mPlum, NLuc is also highly stable both *in vitro* and *in vivo*, and it retains its enzymatic activity even after a 15-hour incubation at 37°C. This is particularly useful for imaging influenza infections since most cell lines are incubated at this temperature.

Use of Mammalian Expression Vector

pCAGGS is a eukaryotic expression plasmid that was developed in the early 1990's and includes a chicken β -actin promoter. Foreign genes inserted into the pCAGGS plasmid are efficiently expressed, and the system presents a way to quickly validate cloning products or generated segments.⁵⁷ Following synthesis of the PA-reporter gene segments, pCAGGS will be used for a series of expression experiments including western blot and fluorescent microscopy to confirm PA and reporter gene expression in the newly generated constructs. This process will ensure that the PA-reporter products used for reverse genetics and subsequent virus rescue are correct and be useful for optimizing future reporter virus characterization and fluorescent expression experiments.

2.2 – METHODS: CLONING

Generation of the PA-Reporter Constructs

mPlum

The mPlum sequence was isolated via restriction digest from the pCAGGS-mPlum plasmid. The restriction digest set up included 1µl of Nhe1-HF and Sac1-HF (New England Biolabs), 2.2µl of pCAGGS-mPlum DNA (0.57µg/µl), 5µl CutSmart Buffer, and 40.8µl nuclease-free water. An undigested control was set up with 2.2µl of pCAGGS-mPlum DNA (0.57µg/µl), 5µl CutSmart Buffer, and 42.8µl nuclease-free water. The reactions were incubated at 37°C for 18 hours and the products were loaded into a 1% agarose gel and run at 200V for 1 hour (**Figure 5**). The 683bp mPlum DNA band was extracted from the gel and purified using QIAquick Gel Extraction Kit (Qiagen). The mPlum DNA concentration (7.9 ng/µl) was measured with the NanoDrop spectrophotometer ND-1000 (Thermo Fisher Scientific).

Overlap Extension PCR

Oligos containing the terminal 50 nucleotides of PA including the 3'UTR (PA_{t50}), which encode necessary packaging signals, were ordered from IDT (**Appendix**). The oligos were annealed together and diluted with duplex buffer to a final concentration of 50µM. Primers were designed and ordered (IDT) to add a sequence to the 5' end of PA_{t50} that overlaps with the 3' end of mPlum. Similarly, primers adding a 15bp sequence to the 3' end of mPlum were ordered (IDT). Phusion[®] High-Fidelity DNA

Polymerase (New England Biolabs) was used to add the overhanging nucleotides to both segments with the following cycling conditions:

98°C	30 seconds	x35 cycles
98°C	10 seconds	
mPlum = 68°C PAt50 = 64°C	30 seconds	
72°C	1 minute	
72°C	5 minutes	
10°C	Hold	

An overlap extension PCR using Phusion[®] was set up to stitch together the mPlum-OH and OH-PAt50 sequences to generate mPlum-PAt50. The overlap extension PCR results were run on a 1% gel at 200V for 1 hour alongside the negative control, mPlum-OH. The size difference in the top bands indicated that the PCR was successful in generating mPlum-PAt50 (**Figure 6**).

The 2235 base pair PA segment containing the 5' UTR with silent mutations, the GSG linker and the 2A protease was ordered as a gBlocks Gene Fragment from (Integrated DNA Technologies). This segment, now referred to as PA_GSG_2A, was resuspended in TE buffer to a final concentration of 10ng/μl.

Nanoluciferase

A gBlocks[®] Gene Fragment of nanoluciferase containing the terminal 50 nucleotides of the PA segment was ordered from IDT and resuspended with TE buffer to achieve a final concentration of 10ng/μl.

Gibson Assembly

mPlum

The Gibson Assembly technique was used to clone the PA_GSG_2A and mPlum-PAt50 segments into the pCAGGS mammalian expression plasmid. First, Phusion[®] PCR was used to add overlapping nucleotides to both the 5' and 3' ends of PA_GSG_2A and mPlum-PAt50. The pCAGGS-mPlum plasmid was linearized with restriction enzymes NheI-HF and SacI-HF at 37°C for 18 hours and inactivated at 65°C for 20 minutes. The linearized pCAGGS plasmid with mPlum removed was purified from a 1% agarose gel using QIAQuick Extraction Kit (**Figure 7**) and PCR was used to add nucleotides overlapping with the PAmut-2A and mPlum-PAt50 to the 3' and 5' ends, respectively.

The Gibson Assembly reaction was set up with 50ng each of pCAGGS, PAmut-2A, and mPlum-PAt50 with the overlapping regions, Gibson Assembly MasterMix (2x), and nuclease-free water. The reaction was incubated at 50°C for 60 minutes and immediately chilled at -20°C for subsequent transformation. Gibson Assembly products were transformed in NEB 5- α Competent *E. coli* cells provided with the kit. 2 μ l of the assembly reactions were added to tubes containing 50 μ l of the 5- α cells. The samples were mixed gently by flicking and set on ice for 30 minutes. Tubes were heat shocked at 42°C for 30 seconds to allow the DNA to enter the bacterial cells, and then placed on ice for 5 minutes. 950 μ l of room temperature SOC media was added to each tube and transferred to a 37°C shaker at 250rpm for 1 hour. LB agar plates containing 100 mg/ml carbenicillin were warmed to 37°C. 100 μ l of the transformed cells were spread onto the agar plates and incubated overnight at 37°C.

Bacterial colonies were then screened for the Gibson Assembly products of interest. Colonies were grown in overnight cultures of 3ml of LB with 100mg/ml carbenicillin at 37°C. The following day, plasmid DNA was purified using QIAprep Spin Miniprep Kit (Qiagen) and the concentration was measured using the ND-1000 spectrophotometer (Thermo Fisher Scientific). All samples were run on a 1% agarose gel and band size was evaluated. Samples with the appropriate molecular weight were selected for further sequencing analysis using multiple sets of primers specific for pCAGGS and internal sequences of PA and mPlum (**Table 2**). Sequencing was performed by the Genetic Resources Core Facility at the Johns Hopkins University Institute of Genetic Medicine using the Applied Biosystems 3730xl DNA Analyzer. The ZymoPURE™ Plasmid Maxiprep Kit (Zymo Research) was used to amplify the pCAGGS-PA-mPlum Gibson Assembly product verified by sequencing. This maxiprep sample was used in subsequent expression experiments including immunofluorescence following an additional sequencing confirmation.

Nanoluciferase

The NLuc-PAt50 segment was PCR amplified with primers to add an additional 15 nucleotides on both the 3' and 5' ends to overlap with the PAmut-2A and pCAGGS segments, respectively. The PAmut-2A and linearized pCAGGS segments were also PCR amplified to add overlapping regions with the NLuc-PAt50 segment.

The Gibson Assembly reaction was set up using the PCR products with overlapping regions. 50ng of the PCR amplified linearized pCAGGS, 150ng of PAmut-

2A, and 150ng NLuc-PAt50 (all with overlapping regions) were incubated with 10µl of 10x Gibson Assembly MasterMix and 0.5µl of nuclease-free water for 60 minutes at 50°C. Following the reaction, assembly products were immediately chilled at -20°C and transformed in NEB 5-alpha Competent *E. coli* cells as described above for the mPlum transformations. Plasmid DNA was isolated from overnight cultures of selected bacterial colonies and run on a 1% gel for molecular weight verification.

Sanger sequencing was performed on selected samples as described above and the ZymoPURE™ Plasmid Maxiprep was used to amplify the sample with correct sequencing. This sample was verified by sequencing again and used for further expression experiments including Western Blot and the Nano-Glo® Luciferase Assay.

Site-directed mutagenesis of pCAGGS-PA-mPlum

Sanger sequencing of the pCAGGS-PA-mPlum plasmid revealed an additional T nucleotide at base 3,020 within the PA segment. This mutation causes a frameshift downstream that disturbs translation of the correct proteins. The QuikChange Lightning Site-Directed Mutagenesis Kit (Agilent Technologies) was used to remove this additional nucleotide. Two individual mutagenic oligonucleotide primers were designed to include the desired deletion in the middle of the primer, with 15 bases of correct sequence on both sides. The primers used are listed in **Table 1**.

A site-directed mutagenesis mutant strand synthesis reaction was set up containing the mutant forward and reverse primers (2.5ng/µl), dNTP mix, QuikChange

Lightning Enzyme, QuikSolution Reagent, 10x QuikChange Lightning Buffer, and nuclease-free water.

The cycling conditions used were:

95°C	2 minutes	x18 cycles
95°C	20 seconds	
66°C	30 seconds	
68°C	4 minutes	
68°C	5 minutes	
4°C	Hold	

Following thermal cycling, Dpn1 restriction enzyme was added directly to each amplification reaction to digest the parent strand of DNA, leaving only the mutant strand remaining. The reaction mixes were mixed thoroughly and incubated at 37°C for 5 minutes. After Dpn1 digestion, the samples were transformed in XL10-Gold ultracompetent cells (Agilent Technologies). 45µl of cells were added to a pre-chilled 14-ml BD Falcon round-bottom tube and 2µl of beta-mercaptoethanol was added. Cells were incubated with the β-ME for 2 minutes on ice. 2µl of the Dpn1 digested product was added to the tube of cells and incubated on ice for 30 minutes following gentle mixing by swirling. The cells were heat shocked at 42°C for 30 seconds and immediately placed back on ice for 5 minutes. 950µl of pre-warmed (37°C) LB broth was added to the tube and incubated at 37°C for 1 hour with shaking at 250rpm. 200µl of the transformed cells were added to pre-warmed (37°C) LB-carbenicillin agar plates and incubated overnight at 37°C.

Colony Screening and Sequence Analysis

The QIAprep Spin Miniprep Kit (Qiagen) was used to purify plasmid DNA from the site-directed mutagenesis pCAGGS-PA-mPlum samples. The sample DNA were submitted for Sanger sequencing. Sequencing results revealed the G nucleotide at position 3,019 immediately preceding the additional T nucleotide was deleted during the site-directed mutagenesis process, but the additional T mutation remained. However, the deletion of the guanine corrected the frameshift of downstream nucleotides. As a result, there is a W422L mutation in the PA segment (**Figure 8**). The PA segments from 15 other H3N2 sequences were analyzed for this mutation, however the tryptophan at position 422 is conserved throughout all 15 viruses (**Figure 9**). For the sake of timeliness, this W422L mutation was not corrected with further site-directed mutagenesis.

2.3 – METHODS: EXPRESSION VALIDATION

Cell Lines

Madin Darby canine kidney (MDCK) and HEK 293T (293T) cells were cultured in Dulbecco's Modified Eagle Medium (DMEM, Sigma-Aldrich) with 10% fetal bovine serum (FBS, Gibco Life Technologies), 100U penicillin/ml with 100µg streptomycin/ml (Quality Biological), and 2mM L-Glutamine (Gibco Life Technologies) at 37°C with air supplemented with 5% CO₂.

Nano-Glo[®] Luciferase Assay

Activity of the nanoluciferase encoded in the pCAGGS-PA-NLuc plasmid was measured by the Nano-Glo[®] Luciferase Assay System (Promega). Because nanoluciferase is an enzyme, it needs a substrate in order to function and emit light. The Nano-Glo[®] Luciferase Assay System allows detection of luciferase activity in mammalian cells using either a lytic or non-lytic method. In this experiment, the lytic method was used to measure nanoluciferase activity from both intracellular and secreted forms of nanoluciferase. The plasmid pNL1.1-NLuc used as a positive control was generously provided by Andrew Mehle at the University of Wisconsin.

MDCK cells were grown to confluence and transfected in at least triplicate in a 96-well plate using Lipofectamine3000 (Thermo Scientific). Cells were transfected with 0.2µg DNA per well of either the pCAGGS-PA-NLuc plasmid, pNL1.1-NLuc, or Lipofectamine alone as a negative control. Plates were incubated at 37°C, 5% CO₂ for the desired amount of time. At 12, 24, and 48 hours post-transfection (hpt), the plate was

removed from the incubator and allowed to equilibrate to room temperature. The Nano-Glo[®] Luciferase Assay Substrate was added to the Nano-Glo[®] Luciferase Assay Buffer at a 1:50 ratio to generate the Nano-Glo[®] Luciferase Assay Reagent. The reagent was equilibrated to room temperature. 100µl of Nano-Glo[®] Luciferase Assay Reagent was added per well and incubated at room temperature for 5 minutes. Luminescence was measured using the Molecular Devices Filter Max F5 Multi-Mode Microplate Reader with SoftMax Pro 6.4 software.

Western Blot for PA in pCAGGS-PA-NLuc

Western blots were performed to evaluate if PA expression was retained in the generated pCAGGS-PA-NLuc construct. Addition of reporter genes can inhibit expression of PA due to potential protein misfolding. However, detection of PA in this experiment is not necessarily indicative of polymerase activity, since the other polymerase subunits PB1 and PB2 were not co-transfected with the pCAGGS-PA-NLuc plasmid.

293T cells were transfected in suspension at 1×10^6 cells/ml in a poly-L-lysine (Sigma-Aldrich) coated 6-well plate. Cells were transfected with 4µg/well of the pCAGGS-PA-NLuc plasmid with Lipofectamine3000. Plates were incubated at 37°C, 5% CO₂ for 48 hours. Media was replaced after 24 hours. 293T cells were also infected with A/Victoria/361/11 at an MOI of 0.5. Following transfection and infection, cells were washed with PBS supplemented with 100g/L Ca²⁺ and Mg²⁺ (PBS+). Cells were lysed with 400µl RIPA buffer per well containing Halt[™] Protease and Phosphatase Inhibitor

Single-Use Cocktail, EDTA-Free (ThermoScientific). Cells were scraped with a pipet tip and transferred to an Eppendorf tube. A 20-gauge needle was used to homogenize the lysates. Lysates were then centrifuged at 12,000 rpm for 15 minutes at 4°C and supernatants were stored at -20°C for future use.

Isolated cell lysates were thawed and mixed with 4x Laemmli Sample Buffer (BioRad) and 50mM DDT (Pierce). No protein concentration assay was performed because β -actin levels were used to normalize total protein content. Samples were boiled for 5 minutes at 100°C and placed on ice immediately. Samples were then separated on a 4-15% Mini-PROTEAN TGX Precase Gels (Bio-Rad) at 150 volts for 40 minutes. BioRad Precision Plus Blue Only protein ladder was used as a standard.

Gels were transferred to polyvinylidene fluoride Immobilon-FL membranes (PVDF; Millipore) for 1 hour at 100 volts. Ice packs were added to keep the transfer chamber cold to avoid overheating the membranes. Membranes were washed with PBS containing 0.2% Tween-20 (Sigma-Aldrich) and transferred to a blocking buffer solution of PBS, 0.2% Tween-20, and 5% Nonfat Dry Milk (Bio-Rad) at 4°C overnight. The following day, primary antibodies were added to the membrane and incubated on a plate rocker overnight at 4°C. The primary antibodies used were Monoclonal Anti-Influenza A Virus Polymerase Acidic Subunit (PA), Clone F1-2C3 (BEI Resources, NR-31685) diluted in blocking buffer 1:250, and Monoclonal Anti- β -actin diluted in blocking buffer 1:500.

The membranes were washed at 4°C three times for 5 minutes each and incubated with secondary antibodies for 1 hour at room temperature. AlexaFluor 657-conjugated secondary antibodies used included a donkey anti-mouse immunoglobulin G and a donkey anti-rabbit immunoglobulin G at 1:500 and 1:1,000 dilutions, respectively. The membranes were washed again at 4°C three time for 5 minutes each and then imaged. Visualization was performed using the FluorChemQ phosphorimager (ProteinSimple).

Fluorescence Microscopy of mPlum in pCAGGS-PA-mPlum

Vero cells were transfected with the pCAGGS-PA-mPlum generated construct and the pCAGGS-mPlum plasmid as a positive control. Cells were also mock transfected as a negative control. 4µg of plasmid DNA was used to transfect the cells with Lipofectamine3000 in a 6-well plate with 1×10^6 cells/ml in suspension. Two coverslips per well were placed prior to addition of the cells for transfection. Plates were incubated at 37°C, 5% CO₂ for 48 hours with media replaced after 24 hours. After 48 hours, media was removed and cells were washed gently three times with PBS+. 1ml of 4% paraformaldehyde (Affymetrix) was added per well and incubated at room temperature for 15 minutes. The cells were washed again three times with 1ml PBS+ per well. 1ml PBS with 0.2% Triton X-100 (Sigma) was added per well and incubated at room temperature for 15 minutes to permeabilize the cells. Coverslips were carefully mounted onto microscope slides with DAPI.

2.3 – RESULTS

Nano-Glo[®] Luciferase Assay

Nanoluciferase activity was measured in relative light units normalized to mock. At 12, 24, and 48 hpt, the activity levels of nanoluciferase in the pCAGGS-PA-NLuc construct were at least ten-fold higher than those of the positive control pNL1.1-NLuc (**Figure 10**). pCAGGS contains a chicken beta-actin promoter with enhancer activity, and it is likely that the pNL1.1-NLuc plasmid kindly provided by Dr. Mehle has a less active promoter. This Nano-Glo[®] Luciferase Assay will later be used to test the luciferase activity of a rescued influenza reporter virus encoding nanoluciferase.

Western Blot

PA was detected at the expected 83kDa size⁵⁸ in the pCAGGS-PA-NLuc transfected and A/Victoria/361/11 infected cell lysates using anti-PA antibodies (**Figure 11**). β -actin protein (42kDa) served as the positive control and was detected in all of the samples, including the mock transfected cells. Detection of PA in the pCAGGS-PA-NLuc samples indicate that the addition of the NLuc genes to the PA segment does not disrupt translation of the PA protein. Western blots were not performed for pCAGGS-PA-mPlum transfected cells in the interest of time. Because of this, it is possible that there is limited PA expression. For both NLuc and mPlum constructs, the presence of PA alone does not suggest successful polymerase activity. To analyze this, the other polymerase subunits PB1 and PB2 would need to be co-transfected with the PA-reporter plasmids.

Fluorescence Microscopy of mPlum in pCAGGS-PA-mPlum

Fluorescence microscopy was used to determine the expression of the mPlum protein in Vero cells transfected with pCAGGS-PA-mPlum (**Figure 12**). The pCAGGS-mPlum positive control transfected coverslips reveal clear mPlum expression when imaged with the Cy5 channel on the Zeiss M2 microscope. Protein expression appears to be diffuse within the cell and not restricted to the nucleus alone. In the mock transfected coverslips, nuclei were stained blue with DAPI and clearly imaged, but no mPlum was detected with the Cy5 channel. The pCAGGS-PA-mPlum transfected Veros imaged with Cy5 did show some detectable levels of mPlum production. mPlum expression was also seen in cells transfected with the pCAGGS-PA-mPlum construct; although at lower levels than the pCAGGS-mPlum transfected cells. While mPlum levels are visually lower than those produced in pCAGGS-mPlum transfected cells, they are higher than the baseline mock values. Therefore, it appears that the translation of the mPlum protein still occurs when adding the protein encoding genes within the PA segment.

Conclusions

The data presented demonstrate that both mPlum and NLuc activity are present in plasmid DNA expressed constructs containing the reporter genes fused to the PA protein with a self-cleaving protease domain between the two proteins. This indicates that the basic strategy of expressing cleavable reporter genes fused to the PA protein results in efficient reporter gene expression and the presence of full length PA, at least in the case

of the PA-NLuc fusion protein. These positive results allowed us to proceed to the rescue of recombinant viruses expressing the PA-reporter gene fusions.

CHAPTER 3: REPORTER VIRUS CHARACTERIZATION

3.1 – INTRODUCTION

Background

Previously generated influenza reporter viruses have suffered from attenuation *in vivo*, *in vitro*, or both, and do not closely represent modern, currently circulating strains of influenza. The objective of this project was to generate a reporter influenza A virus within the A/Victoria/361/2011 background that encodes for mPlum or nanoluciferase within the PA segment. Once the PA-reporter constructs were successfully validated in the pCAGGS mammalian expression vector (Chapter 2), they were moved into the pHH21 plasmid and used in a 12-plasmid based recombinant virus rescue system.^{59,60} pHH21-PA-reporter plasmids take advantage of the unique restriction digest products following BsaI and BsmBI digestion, which create inserts with the same nucleotide overhangs on both the 5' and 3' ends, allowing a single step ligation process to transfer the PA-reporter genes into the pHH21 plasmid.

Reverse Genetics Approach

All eight segments are required to make a functional virus, but because these segments are negative sense RNA strands, they are noninfectious and cannot be used as templates for translation. Therefore, plasmids expressing viral replication machinery proteins are necessary to include in order to achieve virus protein expression and complete the virus replication cycle. When plasmids encoding the eight influenza segments are transfected into 293T cells, all eight influenza viral RNAs are produced and

assemble into functional viral RNPs. Inclusion of the polymerase-containing replication machinery helper plasmids allows these viral RNAs to be replicated to produce more infectious viral particles.³⁶ This reverse genetics system is effective because the pHH21 plasmids contain pol I promoters, and cellular RNA polymerase I is abundantly expressed in mammalian cells. Moreover, previous literature revealed that 293T cells are easily transfected⁶¹ and are best suited for this reverse genetics approach.

Virus Characterization

Several experiments were performed to characterize rescued influenza A reporter viruses encoding mPlum or NLuc. TCID₅₀ and plaque assays were used to quantify the viral titers, and plaque morphology analysis was used to investigate the size and shape of plaques formed by the recombinant wild-type and reporter influenza viruses. Moreover, the replication kinetics of the generated viruses were investigated through low MOI growth curves on Madin-Darby canine kidney cells (MDCK cells), a standard cell line used to grow influenza A virus. Lastly, the previously described expression experiments including the Nano-Glo[®] Luciferase Assay and immunofluorescence for mPlum were used to verify expression of the reporter genes in the rescued viruses.

3.2 – METHODS

Sub-cloning of PA-reporter gene constructs into pHH21

The PA-reporter constructs were sub-cloned out of pCAGGS and into the pHH21 plasmid for use in a reverse genetics system to rescue the reporter virus. BsaI restriction enzyme sites were added to the 3' and 5' ends of the PA-reporter segments with PCR. PCR products were run on a 1% gel and purified using the QIAquick Gel Extraction Kit (Qiagen) (**Figure 13**). The purified reporter plasmids were digested with BsaI at 37°C for 18 hours and heat inactivated for 20 minutes at 65°C. An empty pHH21 plasmid was also cut with BsmBI for 18 hours at 55°C and heat inactivated for 20 minutes at 80°C. Digested products were verified on a 1% agarose gel and purified as described above (**Figure 14**).

The isolated PA-reporter segments were ligated into the linearized pHH21 plasmid at a 3:1 molar ratio for 16°C overnight. Ligations were then transformed in dH5- α cells (ThermoFisher Scientific). 1 μ l of ligation products were added to a 50 μ l aliquot of thawed cells on ice and incubated for 30 minutes. Cells were heat shocked for 20 seconds in a 42°C water bath and immediately returned to ice for 5 minutes. 950 μ l of pre-warmed SOC media was added and cells were transferred to a 37°C shaker at 225rpm for 1 hour. 200 μ l of each transformation was spread on a pre-warmed LB-agar-carbenicillin plate and incubated at 37°C overnight. Bacterial colonies were grown in 3ml cultures containing 100mg/ml carbenicillin and LB broth overnight at 37°C.

Plasmid DNA from the bacterial cultures was purified with the QIAprep Spin Miniprep Kit (Qiagen) and the concentration was measured with the ND-1000 spectrophotometer (Thermo Fisher Scientific). Samples were verified by sequencing at the Johns Hopkins University Institute of Genetic Medicine as previously described using pHH21 forward and reverse primers (**Table 2**). The ZymoPURE™ Plasmid Maxiprep Kit (Zymo Research) was used to maxiprep the pHH21-PA-NLuc and pHH21-PA-mPlum samples that were verified by sequencing.

Reverse Genetics and Virus Rescue – Figure 15

293T cells were plated at 3×10^5 cells/ml in a poly-lysine coated 6-well plate and transfected at 60% confluency. Cells were transfected using TransIT-LT1 transfection reagent with the pHH21-A/Victoria/361/11 segment containing plasmids as shown below.

	Plasmid	μg/μl	
pHH21-A/Vic	PA	0.5	
pHH21-PA-NLuc			
pHH21-PA-mPlum			
	PB1	0.5	} “Pol I plasmids”
	PB2	0.5	
	NP	0.2	
	M	0.2	
	NS	0.2	
	HA	0.5	
	NA	0.5	
Protein Expression Plasmids (A/Udorn/72)	PA	0.4	
	PB1	0.5	
	PB2	0.5	
	NP	0.5	

1	2	3	4	5	6
Pol I plasmids	Pol I plasmids	Pol I plasmids	Pol I plasmids	Pol I plasmids	Pol I plasmids
pHH21- A/Vic-PA	pHH21-PA- NLuc	pHH21-PA- mPlum	pHH21- A/Vic-PA	pHH21-PA- NLuc	pHH21-PA- mPlum
Pol I HA (WT)	Pol I HA (WT)	Pol I HA (WT)	-HA and -NA Negative Controls		
Pol I NA (WT)	Pol I NA (WT)	Pol I NA (WT)			

Plates were incubated for 24 hours at 32°C, 5% CO₂. After 24 hours, 4µl N-acetylated trypsin (NAT, Sigma-Aldrich) was added per well for a final concentration of 10µg/ml. Plates were moved to 37°C, 5% CO₂ and incubated for 4 hours. Each well was then overlaid with 500,000 MDCK cells per well resuspended in 100µl OptiMEM and BSA and placed back at 37°C. 1ml of virus containing supernatant was collected from the wells every 24 hours and cytopathic effects were noted. Wells were replaced with 1ml infectious media (IM) containing DMEM with 100U penicillin/ml, 100µg streptomycin/ml (Quality Biological), and 2mM L-Glutamine (Gibco Life Technologies), 30% Bovine Serum Albumin, and 2µl NAT per well. Collected supernatants were stored at -80°C.

Virus Plaque Assay and Clone Isolation

MDCK cells were seeded at 5x10⁵ cells/ml, 2ml/well, in a 6-well plate and grown to confluency at 37°C. Cells were washed with 1ml/well of PBS+ twice and 1ml of DMEM containing 100U penicillin/ml, 100µg streptomycin/ml (Quality Biological), and 2mM L-Glutamine (Gibco Life Technologies) was added. Plates were moved to 37°C while virus dilutions were made.

Virus-containing supernatants from the reverse genetics transfections were removed from -80°C and allowed to thaw at 4°C. Serial dilutions of 10^{-1} , 10^{-2} , 10^{-3} , 10^{-4} , and 10^{-5} were made in a 24-well plate containing IM with 5µg/ml NAT. Cells were removed from the incubator and infected with 250µl of the appropriately diluted virus inoculum and placed at 37°C for 1 hour with gentle agitation every 15 minutes. Meanwhile, a 1% agarose medium was prepared from equal volumes of 2% agarose (UltraPure Agarose, Invitrogen) in ddH₂O and MEM (Gibco Life Technologies) containing 2% Penicillin and streptomycin, GlutaMAX (Gibco), Bovine serum albumin, and 100mM HEPES (Gibco). N-acetylated trypsin (Sigma) at a concentration of 5µg/ml was added. After 1 hour, the inoculum was removed from the cells completely, and 2ml of the 1% agarose medium was added per well. Plates were incubated at 37°C for 3-4 days until plaque formation was observed.

Virus clones were isolated by picking plaques using a 2ml aspirating pipette tip and agarose plugs were transferred to tubes containing 1ml IM with 5µg/ml NAT. The tubes were placed at 4°C for 1 hour to allow the virus inoculum to seep out of the agarose and into the media. To generate seed stocks from the picked virus clones, MDCK cells were infected in a T25 flask at 100% confluency. 1ml of the purified virus inoculum was added to the flask and incubated at 37°C for 1 hour with gentle rocking every 15 minutes. After 1 hour, 5ml of fresh IM with 5µg/ml NAT was added to the T25 flask and placed at 37°C for two to four days until cytopathic effect was observed. The virus-containing supernatant constitutes the seed stock of each virus, and was collected and stored at -80°C.

Viral RNA Isolation

Viral RNA from the generated seed stocks was isolated using the QIAamp Viral RNA Mini Kit (Qiagen). One-step RT-PCR using PA segment-specific primers was performed in order to generate amplified cDNA from the purified RNA. The cDNA was sequenced as previously described, using primers listed in **Table 2**.

TCID₅₀ Assay

MDCK cells were plated at 1×10^5 cells/ml, with 100 μ l/well in 96-well plates and grown to confluency at 37°C, 5% CO₂. Virus seed stocks were removed from -80°C and thawed at 4°C. Meanwhile, the 96-well plates were washed twice with 100 μ l/well of PBS+. 180 μ l IM and 5 μ g/ml NAT were added per well and plates were moved to 37°C. Serial dilutions of the virus seed stocks were made and respective dilutions were added to the 96-well plates and replaced at 37°C, 5% CO₂ for 5 days. On the fifth day, 75 μ l of 4% paraformaldehyde was added per well for 3 hours to fix the cells. The supernatant-paraformaldehyde solution was removed from the wells and 100 μ l of Naphthol Blue-Black stain was added per well and incubated at room temperature overnight. Plates were washed with tap water, dried, and TCID₅₀ values were calculated using the Reed-Muench method.⁶²

Plaque Morphology

Seed stock plaque morphology was examined by infecting confluent MDCK cells in 6-well plates as described above (page 35). Plates were incubated at 37°C, 5% CO₂ for

4 days and then fixed with 1ml 4% paraformaldehyde/well overnight at room temperature. Following fixation, a micro-spatula was used to remove the agarose plug from each well, and 1ml of Napthol Black-Blue stain was added per well overnight at room temperature. Plates were washed with tap water, dried, and plaques were visualized. Plaque images were taken using an Olympus DP-70 color camera attached to a Nikon Dissection Stereoscope using a total magnification of 10x at the Institute for Basic Biomedical Sciences Microscope Facility within the Johns Hopkins University School of Medicine (**Figure 20**). Image J was used to quantify plaque area (**Figure 21**).

Nano-Glo[®] Luciferase Assay

Confluent MDCK cells in 96-well plates were infected with the rA/Victoria-WT and rA/Victoria-PA-NLuc viruses in triplicate with mock infected cells. The viruses were serially diluted in IM with 5µg/ml NAT five-fold across each row, with a 2×10^{-1} dilution of virus in the first column, ending with virus diluted 1.3×10^{-5} in the last column. Plates were incubated at 37°C, 5% CO₂ for 12 or 24 hours before the Nano-Glo[®] Luciferase Assay Reagent was added. Luminescence was measured with the Molecular Devices Microplate Reader and values were normalized to Mock infected wells (**Figure 22**).

Immunofluorescence of rA/Vic-mPlum

MDCK cells were grown to 100% confluence in a 6-well plate with two glass coverslips per well. The cells were infected with rA/Victoria-WT and rA/Victoria-PA-mPlum viruses at a low MOI=0.001. Additional MDCK cells were transfected in

suspension with pCAGGS-mPlum DNA (4 μ g/well) using Lipofectamine3000. Plates were incubated at 37°C, 5% CO₂ with media replaced on the transfected wells every 24 hours. No media replacement was done for the infected wells. At 12, 24, and 72 hours, the cells were washed three times with PBS+ and fixed with 1ml 4% paraformaldehyde per well for 15 minutes. The wells were washed again three times with PBS+ and then permeabilized with PBS+0.2% Triton X-100 for 15 minutes (1ml/well). A humidified chamber was assembled by adding a damp paper towel to the top of a 1,000 μ l pipet tip box filled halfway with water. A sheet of parafilm was placed on top of the paper towel to seal in moisture. After a third round of washes with PBS+, the coverslips were transferred to the humidified chamber. A blocking solution of PBS with 2% normal donkey serum and 0.5% BSA was added to each coverslip at room temperature for 1 hour to limit non-specific antibody binding. Goat anti-H3-Aichi (HA for H3N2) was diluted in blocking buffer 1:200 and added to each coverslip. The coverslips were incubated in this primary antibody at 4°C overnight. After incubation with the primary antibody, the coverslips were washed seven times with 200 μ l PBS-Tween wash buffer. A FITC-conjugated donkey anti-goat IgG secondary antibody was added. The coverslips were incubated with secondary antibody at 4°C for 1 hour. After secondary antibody incubation, the coverslips were washed another seven times with wash buffer and mounted onto microscope slides with 2 μ l mounting media containing DAPI to counterstain the nuclei. Coverslips were sealed with clear nail polish to prevent cells from drying out, and stored at -20°C.

Coverslips were imaged with the Zeiss AxioImager M2 microscope (**Figure 23**). Orientation and initial focusing was performed under the 10x objective before switching to the 40x objective. Fluorescence channel manipulation and image capture were conducted within the Velocity software program. The DAPI (Blue) channel was used to image cell nuclei and refine the focus. Keeping the same field and focus, the channel was switched to FITC (Green) to visualize HA antibody staining. The channel was then switched again to capture images with the Cy5 (Red) channel to detect fluorescence from mPlum protein expression. Images were contrast adjusted using ImageJ and channels were merged to create composite images.

Low MOI Growth Curve

MDCK cells were grown to confluence in 6-well plates and infected with the respective recombinant A/Vic virus at a low MOI = 0.001. Prior to infection, cells were washed twice with PBS+ and the viruses were diluted in IM and 5µg/ml NAT to an MOI of .001. The inoculum was added to the cells and incubated for 1 hour at 37°C, 5% CO₂. After 1 hour, the inoculum was aspirated and cells were washed three times with PBS+. Fresh IM with 5µg/ml NAT was added to each well and incubated at 37°C. At each hour post infection (hpi) designated in **Figure 24**, the media was removed and stored at -80°C for subsequent titrating. Fresh IM with 5µg/ml NAT was added following collection. TCID₅₀ assays were conducted on all the collected supernatant samples.

Graphing and Statistical Analysis

Growth curves were analyzed with a two-way multiple-comparison ANOVA using GraphPad Prism 7 software. Nano-Glo[®] Luciferase Assay experiments were analyzed with a t-test, also performed in Prism 7.

3.3 – RESULTS

Virus Rescue

Cytopathic effects (CPE) were observed in cultures transfected with rA/Vic-WT and rA/Vic-NLuc plasmids at 24 hours post MDCK overlay, but no CPE was observed in the rA/Vic-mPlum plasmid transfected cells until 48 hours. CPE included nuclei enlargement and cell rounding. After 72 hours of incubation, all of the cells transfected with either the rA/Vic-WT or rA/Vic-NLuc plasmids were dead. However, it took until the 96-hour time point to observe complete cell death in the rA/Vic-mPlum transfected cells.

Following RT-PCR of purified viral RNA, Sanger Sequencing analysis demonstrated the seed and working stocks of the rA/Vic-PA-mPlum viruses had the exact sequence that was present in the plasmid used to rescue the viruses, which included the W422L mutation. The sequence of the PA segment of the rA/Vic-PA-NLuc virus was identical to that present in the plasmid used to rescue the recombinant virus. Working stock sequencing data are shown in **Figures 16-18**. This confirms that the recombinant viruses had the expected PA-reporter segment sequence with no additional mutations.

Titers of Generated Recombinant Viruses

The TCID₅₀ value, or the Tissue Culture Infective Dose, is a measurement of the amount of virus needed to kill 50% of cells. The calculated TCID₅₀ values for the working stocks are shown in **Figure 19**. The titer of the rescued rA/Vic-PA-NLuc virus was unexpectedly higher than that of the wild-type rescued rA/Vic-WT, and confirms

that no virus attenuation occurred when the nanoluciferase gene was added to the specific internal region of the PA segment. However, there is a significantly lower titer of the rA/Vic-PA-mPlum virus as compared to either the wild-type or NLuc virus, indicating the virus is somewhat attenuated.

The viral titers calculated via plaque assay were consistently approximately 1 log value lower than the TCID₅₀ calculated value (**Figure 19**). Despite the lower titers of the mPlum rescued virus, there were no differences in the calculated plaque areas (**Figure 21**), and both reporter viruses formed plaques with the same morphology as the wild-type virus (**Figure 20**). However, it took an additional two days for the rA/Vic-PA-mPlum virus to reach these sizes, indicating there was an attenuation in the ability of the virus to form plaques.

Nano-Glo[®] Luciferase Assay

Nanoluciferase activity was confirmed at both 12 and 24-hour post-infection using the Nano-Glo[®] Luciferase Assay (**Figure 22**). Both rA/Vic-WT and mock infected MDCK cells had very low, nearly undetectable levels of luminescence after all luminescence readings were normalized to mock infected wells. The higher relative light unit (RLU) value of the 12hpi timepoint in comparison to 24hpi with rA/Vic-PA-NLuc is likely due to cell death at 24hpi. These results verify activity of the nanoluciferase enzyme encoded in the rescued rA/Vic-PA-NLuc reporter virus.

Immunofluorescence of rA/Vic-mPlum

At 12hpi, HA antibody staining was observed in both rA/Vic-WT and rA/Vic-PA-mPlum infected cells, with fewer infected cells detected in the rA/Vic-PA-mPlum infections. Infected cells expressing the H3 HA surface glycoprotein appear as green cells when imaged with the FITC channel. **Figure 23** shows the DAPI, FITC, and Cy5 merged channels for the MDCK infections with mock, rA/Vic-WT and rA/Vic-PA-mPlum, respectively. At 12 and 24hpi, no mPlum protein was detected under the Cy5 channel. At 72hpi, all of the cells infected with either the mPlum reporter or wild-type virus had died, and none were successfully counterstained with DAPI. **Figure 23** also shows the successful positive control transfection of pCAGGS-mPlum at 24hpt, as well as the inability to detect mPlum expression in the 24hpi rA/Vic-PA-mPlum infected MDCK cells. This experiment will be repeated with additional time points at 36 and 48hpi in order to try and capture mPlum expression prior to cell death. The results at 12hpi however, confirm that the mPlum reporter virus rA/Vic-PA-mPlum is infectious and produces virus particles with HA surface glycoprotein, even though no mPlum fluorescence is detectable.

Low MOI Growth Curve

The rA/Vic-WT and rA/Vic-NLuc viruses reached peak viral titers of 5.4 and 4.3 log TCID₅₀/ml at 48 hpi, respectively (**Figure 24**). These two viruses grew with similar kinetics, and the greater titer of rA/Vic-NLuc was evident as soon as 24 hpi. In contrast, rA/Vic-mPlum reached a peak viral titer of 5.3 log TCID₅₀/ml at 72 hpi and

demonstrated a delayed ability to produce infectious virus. It also took longer to observe clearance of cells in the TCID50 plates infected with rA/Vic-mPlum, and these plates were fixed with 4% formaldehyde three days later than the rA/Vic-WT and rA/Vic-NLuc plates.

CHAPTER 4: DISCUSSION

4.1 – OVERVIEW

Reporter viruses are useful tools for visualizing replication dynamics, analyzing tissues involved in infection, and screening novel antiviral therapies. In this project, two influenza A reporter viruses were generated using the mPlum fluorescent protein and the luciferase nanoluciferase in the backbone of the A/Victoria/361/11 H3N2 strain. Based off previously published work by Andrew Mehle and colleagues, the reporter genes were inserted into the PA segment and packaging signals were moved to the end of the coding region to ensure full translation of the fluorescent protein.

4.2 – rA/Vic-mPlum

Despite rescue of both the recombinant mPlum and nanoluciferase encoding viruses, rA/Vic-mPlum exhibited significant attenuation *in vitro*, reaching significantly lower peak viral titers as compared to the wild-type A/Vic rescued virus. In addition to reaching lower peak viral titers, rA/Vic-mPlum took longer to demonstrate cytopathic effects in infected MDCK cells. Plaques also took longer to form, though they eventually grew to the same size as those of rA/Vic-WT. Furthermore, at 12 and 24-hours post-infection, no mPlum protein was detectable with immunofluorescence microscopy, despite signs of infection. This is in contrast to the fact that mPlum was detected after transfecting cells with plasmids encoding the PA-NLuc protein. This may be due to decreased transcription and/or translation of the mPlum coding region in virus infected cells or reduced stability of the mPlum protein when expressed from the PA gene

segment in the context of virus infection. However, the production of a replication-competent virus indicates that there is successful incorporation of the PA segment into the influenza viral particles, since it is required as part of the polymerase machinery. The packaging signals for the PA segment were moved to the end of the mPlum gene, so it is possible that there was full transcription and translation of the mPlum protein, but levels are too low to detect with immunofluorescence. Sequence analysis of the working stocks used for MDCK cell infections verified the continued expression of the reporter gene despite the few rounds of passaging between plaque purification, seed stock, and working stock generation. Despite correct sequencing, it is possible that replicating viruses during the MDCK cell infections used in immunofluorescent imaging were lost, and more fit wild-type-like viruses emerged as the dominant virus.

The attenuation of the rA/Vic-mPlum virus may point to the importance of reporter gene size when constructing influenza A reporter viruses. The mPlum fluorescent protein is 681bp, while nanoluciferase is 513bp. According to the experiments performed in this thesis, even this 168bp difference may be enough to disturb viral replication kinetics. Despite the size differences between mPlum and nanoluciferase, it is possible that the mPlum protein interferes with the formation of the polymerase resulting from interactions between PA, PB1, and PB2. No analysis of charge differences or spatial analyses was performed, but may be useful in elucidating the challenge with using mPlum as a reporter gene in this context.

Another challenge faced with the rA/Vic-mPlum reporter virus is use of mPlum as a far-red monomeric protein. Inherently harder to detect via microscopy than fluorescent

proteins with shorter wavelengths, the mPlum protein has a brightness of 4,100 compared to other frequently used proteins in this spectrum such as mRaspberry (12,900) and E2-Crimson (28,900).⁶³ Moreover, PA expression for the pCAGGS-PA-mPlum construct was not performed, and attempts to stain for PA during transfection-based immunofluorescence experiments in Vero cells were obscured by high levels of non-specific antibody binding. The W422L mutation in the PA region of pCAGGS-PA-mPlum is also an additional concern and may have a deleterious effect on expression of PA or mPlum.

Despite the inability to detect mPlum expression in infected MDCK cells and the lower replication kinetics of the rA/Vic-mPlum virus, the rescue of this reporter virus suggests that smaller and brighter fluorescent proteins should be considered for more useful applications of influenza A reporter viruses.⁶⁴

4.3 – *rA/Vic-Nluc*

When compared to rA/Vic-WT, the rA/Vic-NLuc virus grew to higher titers in MDCK cells but formed plaques of equivalent size in the same time period. This suggests that the rA/Vic-NLuc virus replicates at least as well, and perhaps better, than its parental virus. The reason for this increased infectious virus production is not clear and should be investigated more carefully. The other viral RNA segments should be sequenced to ensure that no mutations were acquired that might be leading to increased virus replication. In addition, the replication dynamics of rA/Vic-NLuc should be compared to

rA/Vic-WT viruses used in alternate virus rescue experiments to see if the lower titer of rA/Vic-WT was specific to this project.

The rescue of the rA/Vic-NLuc virus was successful and suggests a range of future imaging applications. First, it is possible to use the generated pHH21-PA-NLuc plasmid in additional 12-plasmid based reverse genetics approach. As such, segments from circulating influenza strains can be isolated and sub-cloned into pHH21, where the pHH21-PA-NLuc plasmid can be used in place of the circulating strain's PA segment. Products from the reverse genetics approach would yield nanoluciferase-expressing viruses where seven of eight segments match circulating strains, with limited differences in the PA sequence. By constructing the rA/Vic-NLuc virus in an H3N2 background from 2011, this reporter virus is more useful for investigating currently circulating H3N2 strains than the previously generated nanoluciferase reporter virus by Tran et. al., which used a 1933 strain of H1N1.

4.4 – FUTURE DIRECTIONS

Overview

Nanoluciferase-based reporter viruses could be used to analyze circulating influenza viruses in novel ways. For example, the reporter virus may serve as an alternate method for screening antibody neutralization capabilities. Luminescent output is also a more easily quantifiable method than CPE scoring that is typically done with antibody neutralization assays. Similarly, the efficacy of new antiviral drugs can be quickly tested *in vitro*, where cells are infected with the reporter virus. However, the use of an enzyme

like nanoluciferase in construction of a reporter virus does have its limitations. Primarily, the substrate for the enzyme cannot always be administered systemically, so animal model-based imaging experiments are limited. In these cases, fluorescent proteins such as mPlum would lend more extensive options and should continue to be explored.

Live-Cell Imaging

While static imaging of cells infected with the rA/Vic-reporter viruses revealed successful infection (rA/Vic-mPlum) and production of nanoluciferase (rA/Vic-NLuc), these viruses can be used in further live imaging experiments. For example, once expression of mPlum protein is validated in rA/Vic-mPlum, infection of primary human nasal epithelial cells (hNEC) with rA/Vic-mPlum may inform the mechanism behind viral spread. The use of hNEC cultures, rather than traditional cell lines, preserves the mucus production and ciliary motion present in the human respiratory tract. Live imaging the infection of these primary hNECs with the rA/Vic-mPlum reporter virus can help deduce the importance of mucociliary spread of IAV in comparison to cell-to-cell spread through various cellular networks.⁶⁵

Seasonal Influenza Transmission Dynamics

The generated rA/Vic-NLuc reporter virus can also be used for tracking virus infection *in vivo* through bioluminescent microscopy and provides a unique approach to investigating infection and transmission dynamics of seasonal influenza viruses.

Recently, a nanoluciferase-encoding IAV with the pandemic 2009 H1N1 influenza virus

background was recently used to infect ferrets and evaluate viral dynamics in real-time.⁶⁶ Results demonstrated that bioluminescent imaging in the ferret model was highly sensitive and significantly correlated to viral titers of collected nasal washes. The rA/Vic-NLuc produced in this project can be used in a similar fashion to further investigate the viral transmission and replication dynamics of modern H3N2 viruses.

Serum Antibody Neutralization Alternative

These generated IAV reporter viruses also offer an alternative approach to standard serum antibody neutralization assays (NT). NT assays measure the titer of antibodies necessary to block cytopathic effects caused by the virus, through inhibiting viral fusion and entry into the cell.⁶⁷ While these assays provide a reliable method for determining antibody concentrations, NT assays are more time-consuming, expensive, challenging to standardize between laboratories, and require the use of live virus that induces cytopathic effects.⁶⁸ The only widely accepted alternative to NT assays are hemagglutinin inhibition (HI) tests, which are more affordable and easier to standardize,⁶⁹ but less sensitive and subject to misinterpretation by the investigator. Use of an IAV reporter virus offers a unique alternative to standard NT and HI assays, and may provide a more rapid and affordable method for determining antibody neutralization titers. For example, the PA-NLuc segment based of the A/Victoria H3N2 virus that was generated in this project can be used in a reverse genetics approach with segments isolated from currently circulating or historical strains of influenza, to make additional reporter viruses. MDCK cells can be infected with these reporter viruses in the presence

of isolated serum. Following incubation, addition of the NLuc substrate will allow the luminescent output to be used as a rapid quantitative measurement of virus neutralization. This is less time-consuming than standard downstream ELISA used in NT assays, and will help detect a broader range of neutralizing antibodies than those only against HA epitopes as in the case of HI assays.⁷⁰

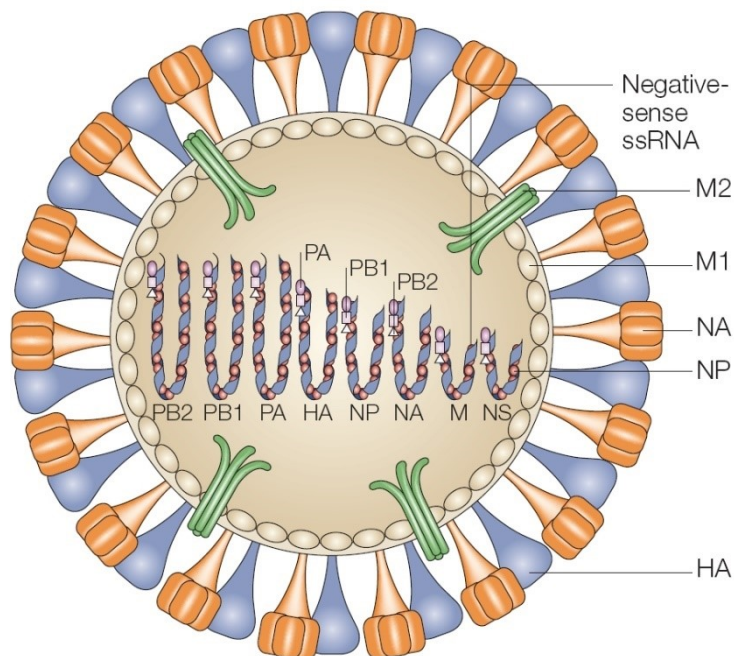


Figure 1: Influenza virus structure. Adapted from Horimoto, *Nature Reviews Microbiology*, 2005.⁷¹

IAV has eight internal gene segments that replicate independently of one another in an infected cell. The surface of the virus particle is decorated with glycoproteins hemagglutinin (HA) and neuraminidase (NA).

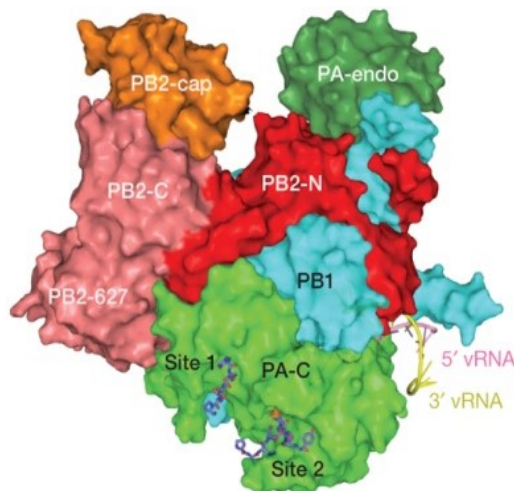


Figure 2: The structure of the influenza A polymerase complex. Adapted from Lukarska, *Nature* 2017.⁷² The complex is created with interactions between the subunits PA, PB1, and PB2.

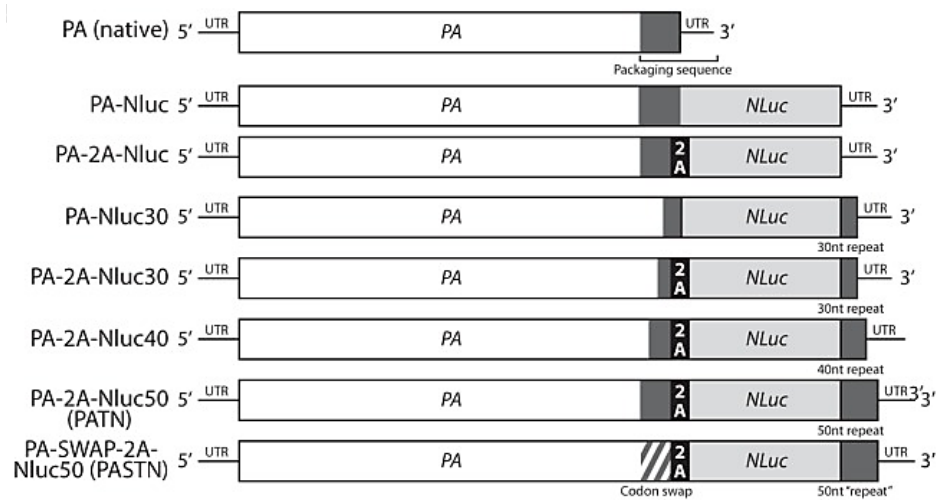


Figure 3: PA-SWAP-2A-NLuc50 (PASTN) construct by Tran et al.⁵² This construct served as the basis for the recombinant A/Victoria H3N2 reporter viruses generated in this project.

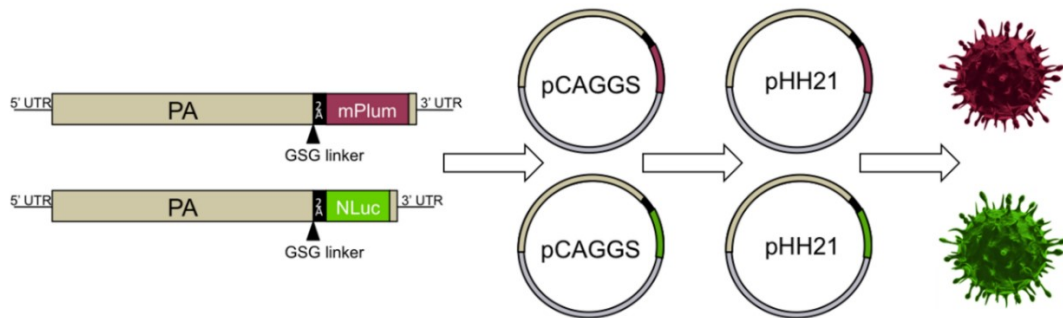


Figure 4: Project outline. PA-reporter constructs were first generated and moved into the pCAGGS mammalian expression plasmid. Following confirmation of expression, the PA-reporter constructs were subcloned into the pHH21 plasmid and used in a reverse genetics approach to generate complete influenza reporter viruses.

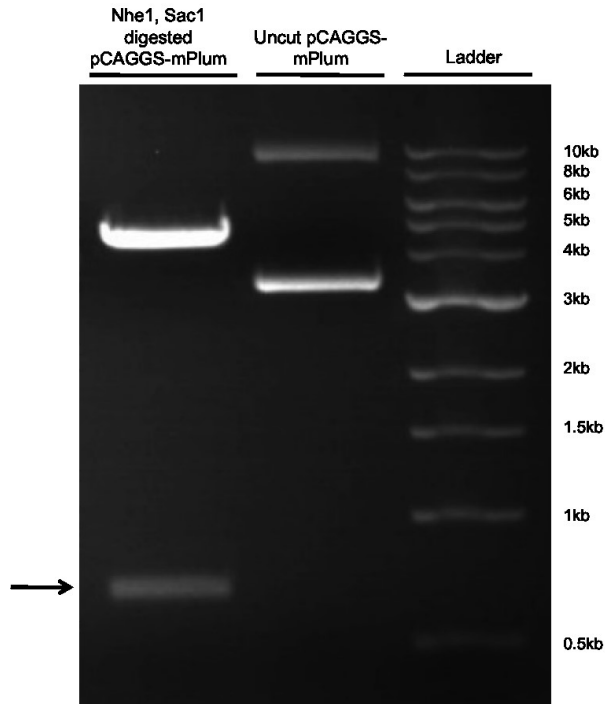


Figure 5: Restriction enzyme digestion of pCAGGS-mPlum. pCAGGS-mPlum plasmid DNA was digested overnight with restriction enzymes Nhe1 and Sac1 and products were run on a 1% agarose gel. The mPlum fragment at 681bp (arrow) was extracted from the agarose gel and purified.

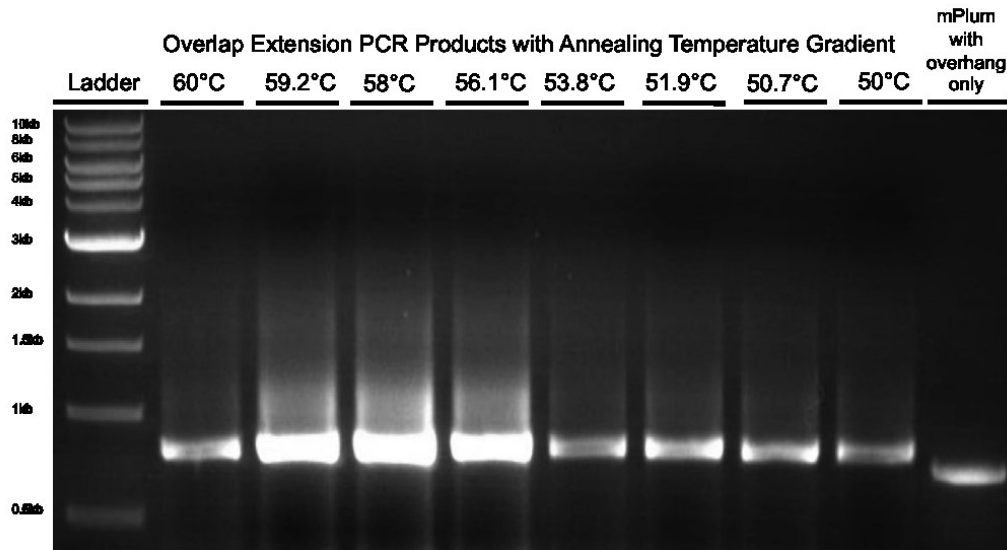


Figure 6: Overlap extension PCR for the addition of PA terminal 50 nucleotides to mPlum. The mPlum-OH and OH-PAt50 sequences were stitched together using a Phusion®-based overlap extension PCR. A gradient from 50-60°C was used to determine the optimum annealing temperature of 58°C. The negative control lane “mPlum with overhang only” indicates sample without the additional terminal 50 nucleotides of PA added. The molecular weight differences between this band and all other samples indicate successful joining of the two segments.

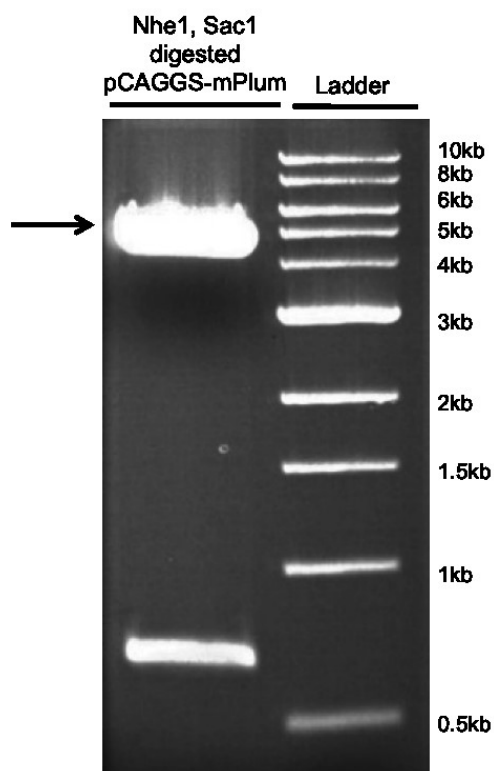


Figure 7: Restriction enzyme digestion of pCAGGS-mPlum for the generation of linearized pCAGGS. The pCAGGS-mPlum plasmid was digested overnight with Nhe1 and Sac1 an additional time, and the top band containing linearized pCAGGS alone (arrow) was extracted and purified. The mPlum band at 681bp was discarded. The purified pCAGGS DNA was then used for Gibson Assembly of pCAGGS, PA, and mPlum.

Table 1: Primer Sequences

mPlum_Forward	CATGGTGAGCAAGGGCGAG GAGGTCA	Add overhanging segments and stitch together the mPlum and terminal 50 nucleotides of PA
mPlum_Rev_PAt50 overhang	GAACCAAGACGCATTGAGC ACTTAGGCGCCGGT	
mPlum_Reverse	CTTAGGCGCCGGTGGAGTGG CGGCCCTC	
PA_terminal50_mPlum overhang For	CTCCACCGGCGCCTAAGTGC TCAATGCGTCTTG	
PA_terminal50_rev erse	AGTAGAAACAAGGTACTTTT TTGGACAGTACGGAT	
PA_mPlum_Rev	GCTCACCATGGGGACCGGG GTTTTC	Prepare gBlock of PA_GSG_2A for pCAGGS Gibson Assembly with mPlum
pCAGGS_PA_For	GCAAAGAATTCGAGCTGAA AGCAGGTACTGATTCAAAT G	
mPlum_PA_For	GGTCCCCATGGTGAGCAA GGGCG G	Prepare mPlumPAt50 for pCAGGS Gibson Assembly with PA_GSG_2A
pCAGGS_mPlum_Rev	GGAAAAAGATCTGCTAGAG TAGAAACAAGGTACTTTTTT GG	
mPlum_PA_Rev	AGTAGAAACAAGGTACTT TTTTGGAC	Used with mPlum_PA_For to amplify the mPlumPAt50 segment
2A_mPlum_For	CGGTCCCATGGTGAGCAAG GGCGAG	Used to stitch together the mPlum-PAt50 and rest of the PA segment
mPlum_2A Rev	GCTCACCATGGGACCGGGGT TTTCT	
Site-Directed Mutagenesis del3020 Forward del3020 Reverse	Forward: GAGCTAACTGATTCACTCTG GATAGAGCTCGATGAAATTG Reverse: CAATTTTCATCGAGCTCTATC CAGACTGAATCAGTTAGCTC	Delete the additional T nucleotide at position 3019 in the PA segment of pCAGGS-PA-mPlum
PAGSG2A_NLuc_Rev	TGAAGACCATGGGACCGGG GTTTTC	Prepare gBlock of PA_GSG_2A for pCAGGS Gibson Assembly with NLuc (with pCAGGS_PA_For)
NLuc_PAGSG2A_For	CCCCGGTCCCATGGTCTTCA CACTCGAAG	Prepare gBlock of NLucPAt50 for pCAGGS Gibson Assembly with PA_GSG_2A

Table 2: Sequencing Only Primers

PA FluA9 R	ATACGTCTCGTATTAGTAGAAACAAGGTACT
PA FluA10 F	CGACGTCTCCGGGAGCGAAAGCAGGTACTG
H3PA_1750_R	TCATTTTGACCTTTGATGTTCCGT
H3PA_1646_F	TGGGAGAAATACTGTGTCCTTGAGATA
H3PA_1525_R	TCGCCTTCCCTCTTTAGTTCTGCACTTGC
H3PA_1748_F	CTGGATAGAGCTCGATGAAATTGGAGA
H3PA_1326_R	CCCTTCTCCTTCGTGACTTGGGTCTTC
H3PA_771_F	AGCTTTCTCAAATGTCCAAAGAAGTGA
H3PA_587_R	TGGCCATTTCTTGTCTTATGGTAAACA
H3PA_395_F	GGAGAGAAGTCCACATATATTACCT
pHH21-1 F	GGTATATCTTTCGCTCCGAG
pHH21-2 R	CACTTTCGGACATCTGGT

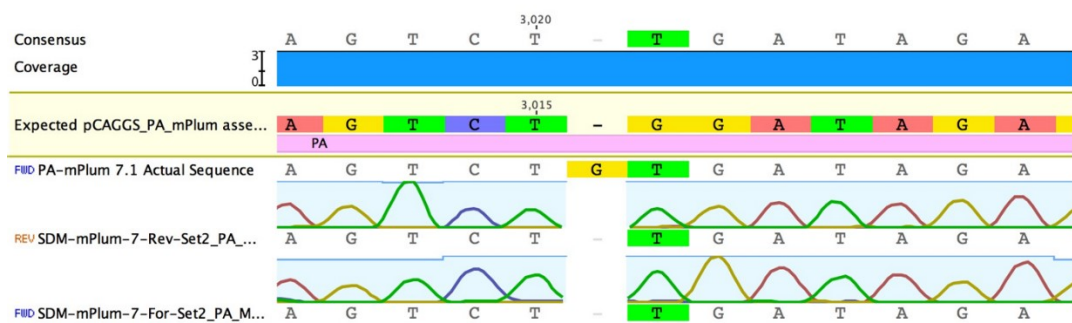


Figure 8: Sequence alignments showing frameshift mutation in pCAGGS-PA-mPlum. A mutation from a G to a T within the PA region of the pCAGGS-PA-mPlum construct results in a frameshift. After site-directed mutagenesis, the G nucleotide preceding the G→T mutation was deleted, effectively fixing the frameshift mutation, but creating a W422T mutation in the PA region.



Figure 9: Sequence alignments of PA segments of multiple H3N2 strains show conserved tryptophan at position 422. Fifteen PA sequences from H3N2 viruses since 1971 were obtained through GenBank. Alignment of these sequences indicates conservation of the tryptophan at position 422 as compared to the W422T mutation observed in the pCAGGS-PA-mPlum generated plasmid (sample #10 – SDM7 maxi).

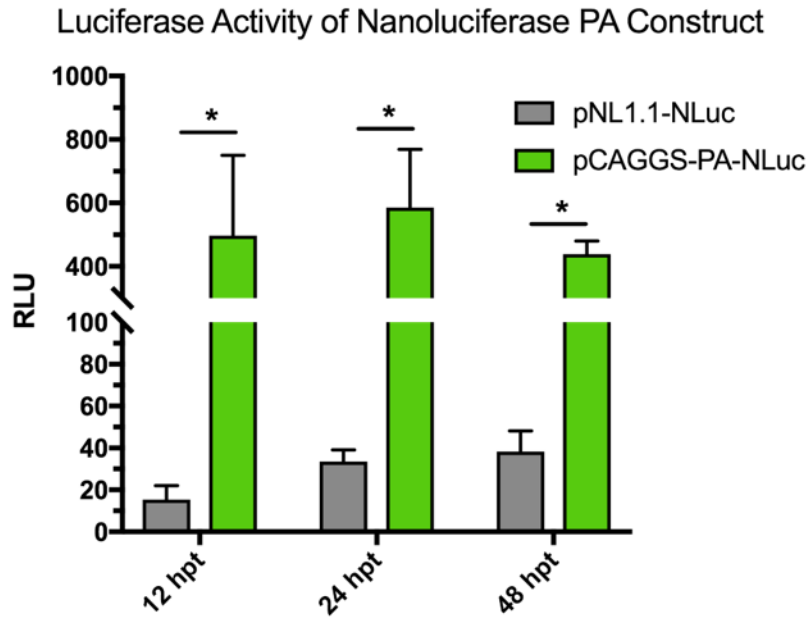


Figure 10: Validation of nanoluciferase expression of pCAGGS-PA-NLuc. Nano-Glo[®] Luciferase assay was used to detect luminescence in Vero cells transfected with the pCAGGS-PA-NLuc plasmid at 12, 24, and 48 hours post transfection. Experiments were conducted twice with nine replicate wells per sample and representative data are shown. Error bars indicate standard deviation. * denotes statistically significant differences ($p < 0.05$) in the luminescence output (RLU) as compared to the positive control pNL1.1-NLuc transfected cells, evaluated by t-test.

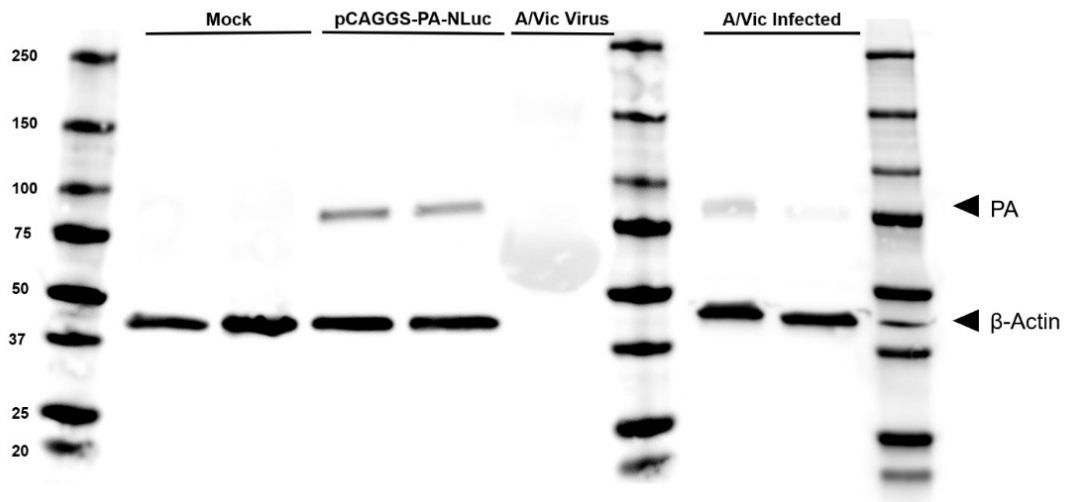


Figure 11: Validation of PA protein expression in pCAGGS-PA-NLuc. Western blotting of Vero cells transfected for 48 hours with pCAGGS-PA-NLuc revealed successful detection of PA (~75kDa). Vero cells were also infected with a laboratory stock of A/Victoria/361/2011. Protein levels were normalized with beta-actin (40 kDa). The image shown includes two replicates per sample with the exception of the well with heat-killed A/Vic virus only. Previous attempts to detect PA with alternate antibodies in either A/Vic infected or pCAGGS-PA-NLuc transfected Veros or 293T cells was unsuccessful.

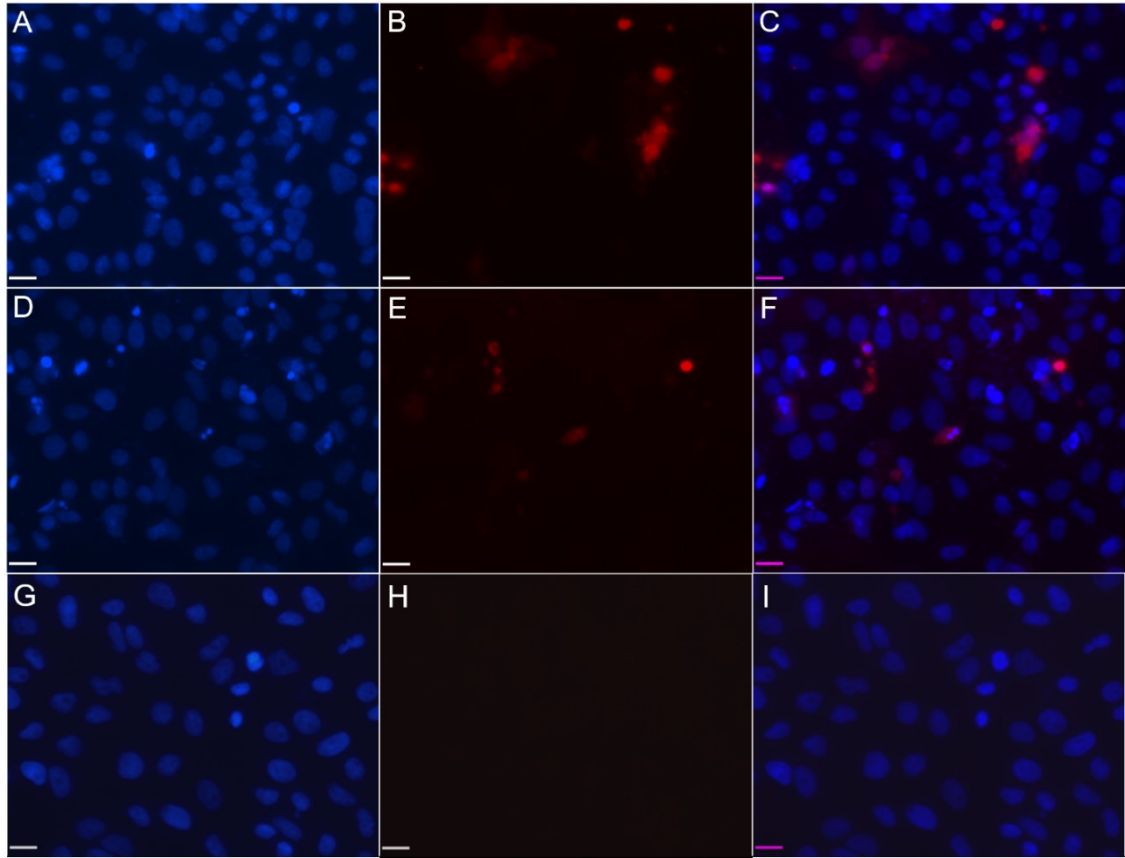


Figure 12: Fluorescence microscopy of mPlum expression in pCAGGS-PA-mPlum. Vero cells transfected with pCAGGS-mPlum (A-C), the generated pCAGGS-PA-mPlum plasmid (D-F), and mock (G-I). Imaged at 48hpt, 40x magnification, and counter stained with DAPI. mPlum protein production is observed in both the positive control pCAGGS-mPlum transfections and the pCAGGS-PA-mPlum transfections.

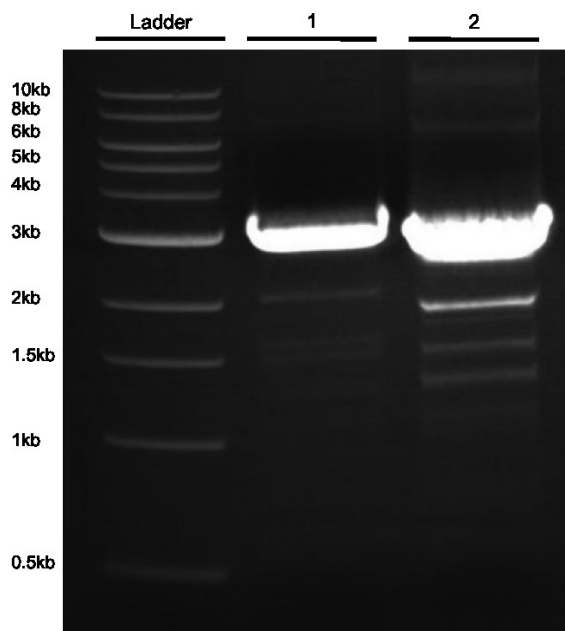


Figure 13: Addition of BsaI restriction sites to PA-mPlum and PA-NLuc constructs by PCR. BsaI restriction enzyme sites were added to the 3' and 5' ends of the PA-mPlum and PA-NLuc segments using PCR. PCR products of the new BsaI-PA-mPlum (1) and BsaI-PA-NLuc (2) were run on a 1% gel and bands indicated close to 3kb were extracted purified using the QIAquick Gel Extraction Kit (Qiagen).

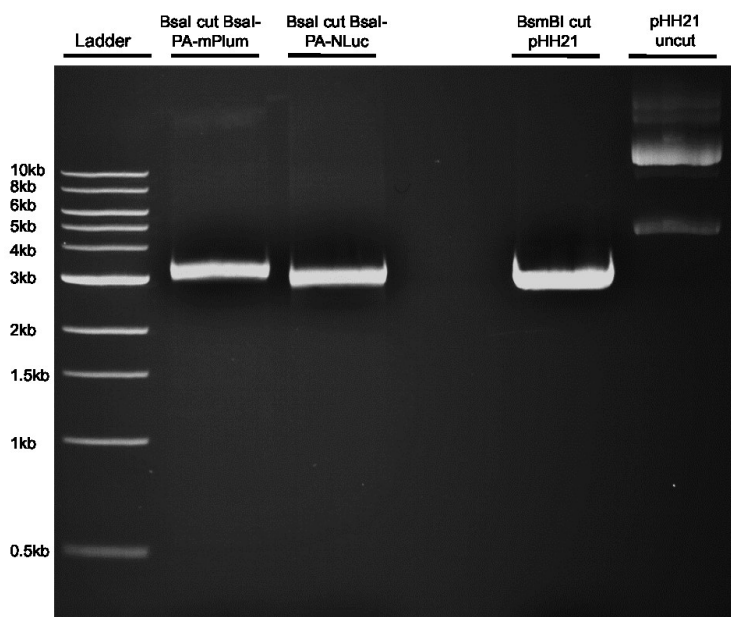


Figure 14: Restriction enzyme digestion of PA-mPlum and PA-NLuc constructs and the pHH21 plasmid. The PCR generated BsaI-PA-mPlum and BsaI-PA-NLuc plasmids were digested with BsaI at 37°C for 18 hours and heat inactivated for 20 minutes at 65°C. An empty pHH21 plasmid was also cut with BsmBI for 18 hours at 55°C and heat inactivated for 20 minutes at 80°C. Digested products were run on the 1% agarose gel.

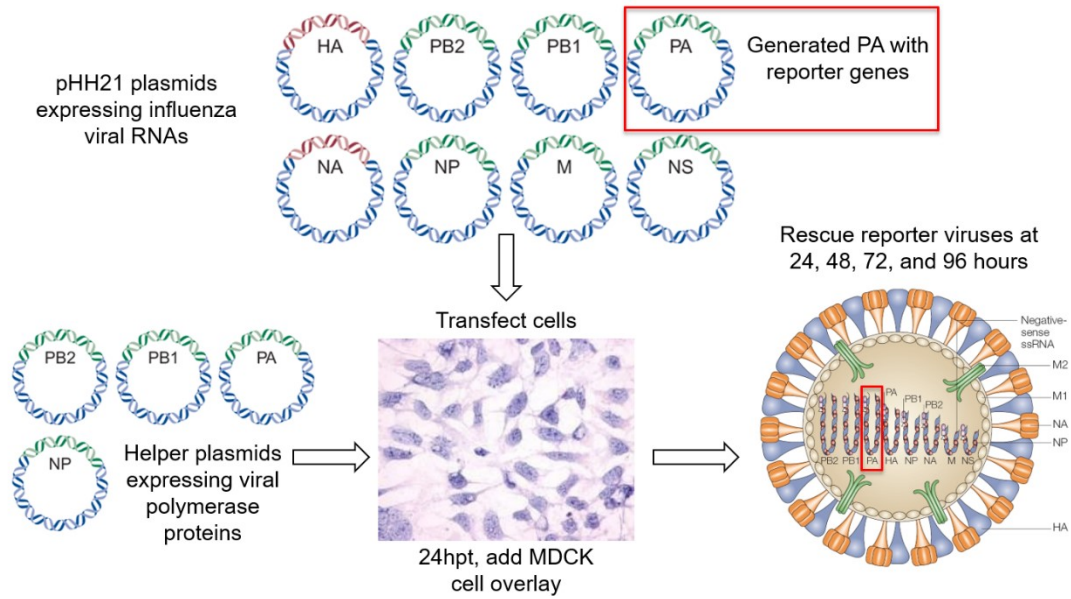


Figure 15: Schematic of the reverse genetics process for creating influenza A viruses. In this process, cells are transfected with plasmids expressing influenza viral RNAs in the presence of helper plasmids. MDCK cells are overlaid and virus-containing supernatant is collected at 24, 48, 72, and 96 hours later. cDNAs encoding the PA, PB1, PB2, and NP helper plasmids are contained in the pCAGGS eukaryotic expression vector with a very active promoter for the purpose of generating large quantities of the influenza RdRp necessary for the replication of viral genomic RNA and the transcription of viral mRNAs. The other influenza segments are cloned into individual pHH21 plasmids that contain a human RNA polymerase I promoter and a mouse RNA polymerase I terminator.^{73,74}

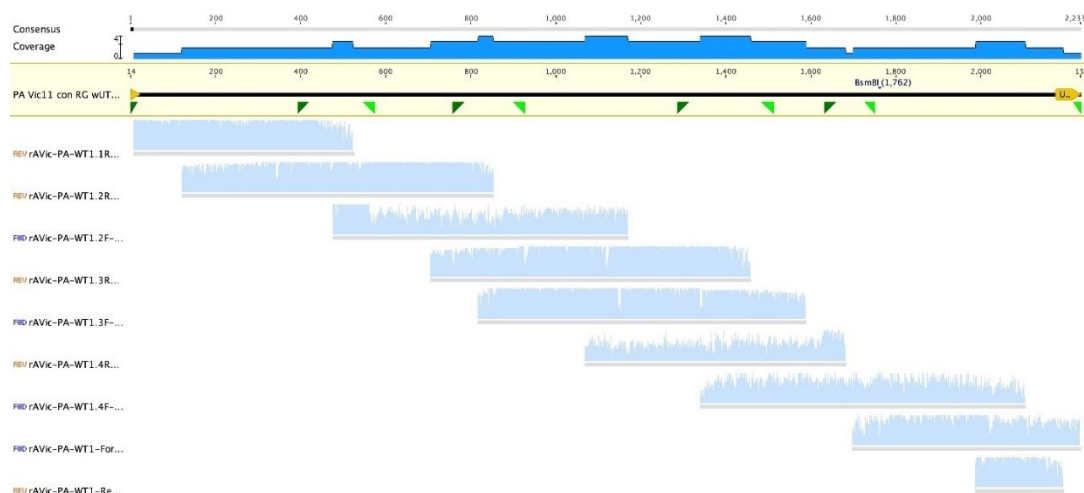


Figure 16: Sequence analysis of the working stock of rA/Vic-WT. No mutations away from the consensus sequence are observed.



Figure 17: Sequence analysis of the working stock of rA/Vic-NLuc. No mutations away from the consensus sequence are observed.

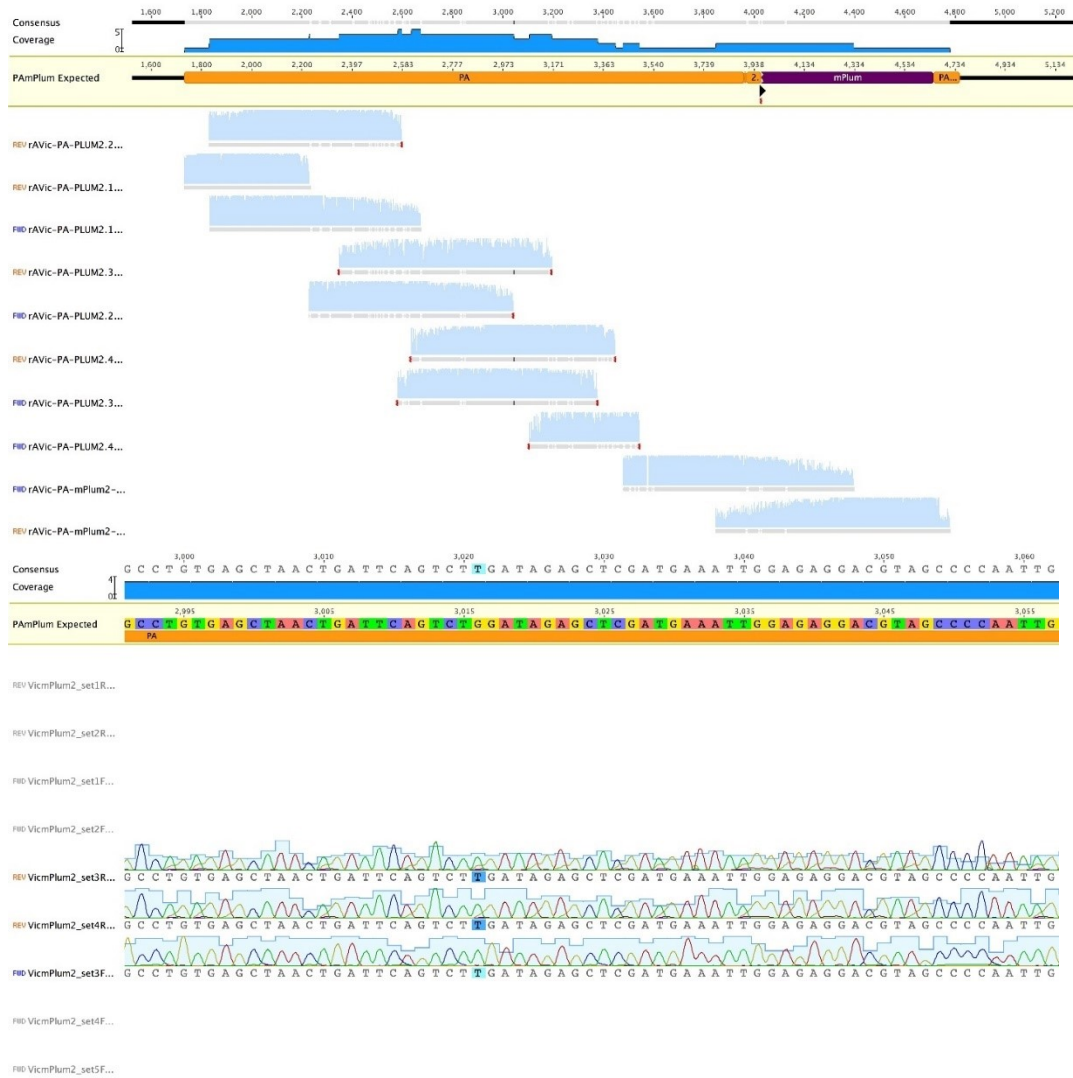


Figure 18: Sequence analysis of the working stock of rA/Vic-mPlum. Sequencing results shows persistence of G3021T mutation within the PA segment. No other mutations are seen from the expected consensus sequence.

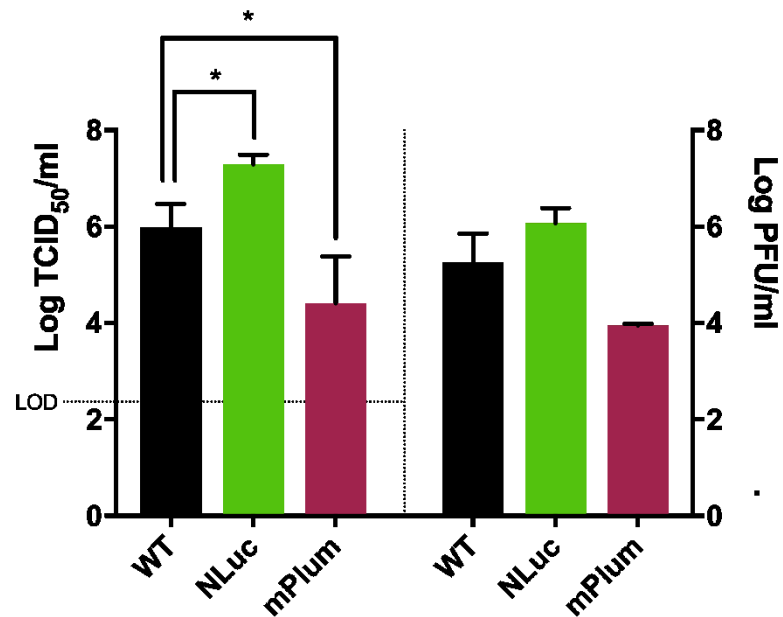


Figure 19: Working stock titers of recombinant A/Vic viruses by TCID₅₀ and plaque assays. TCID₅₀ and plaque assays for the generated viruses were performed on MDCK cells. Log TCID₅₀/ml values represent mean titers across triplicates. Log PFU/ml values represent mean values of two replicate experiments. * denotes statistically significant differences (p<0.05) using a t test.

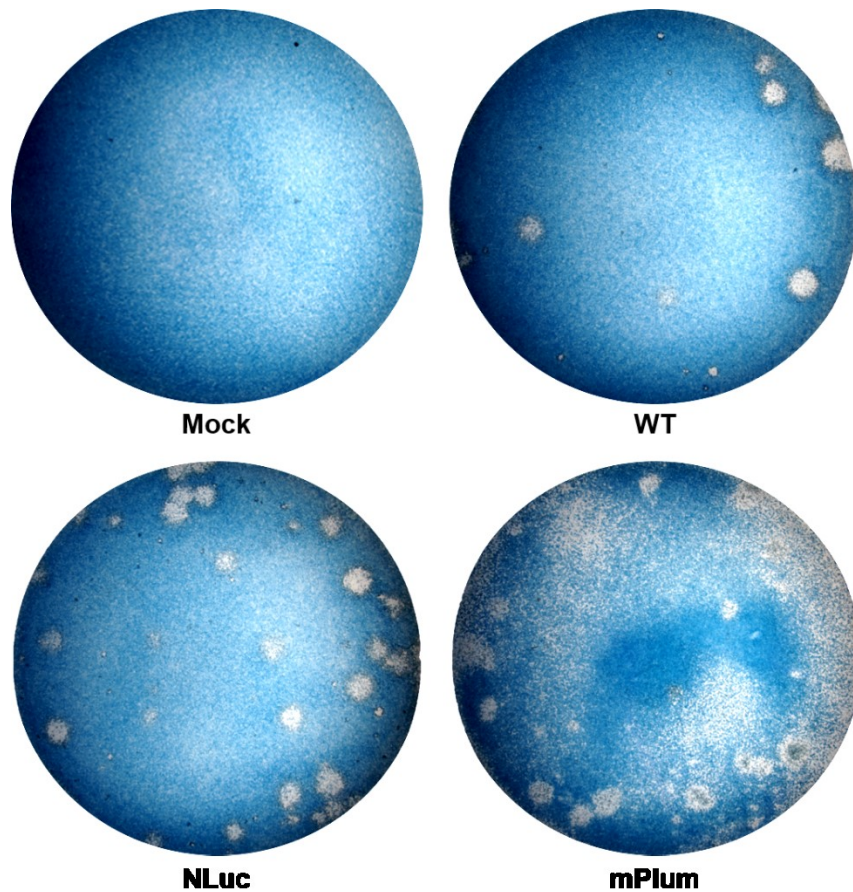
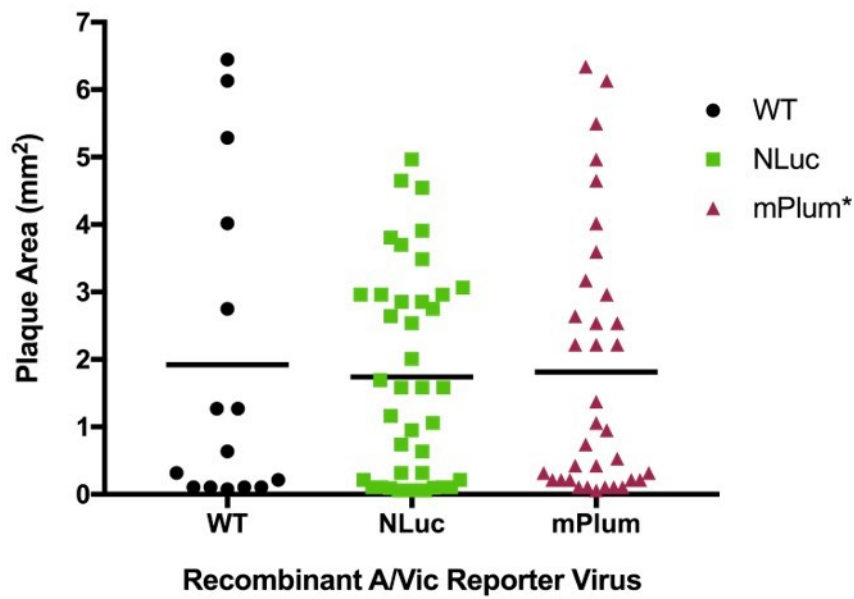


Figure 20: Plaque assay of MDCK cells infected with WT and reporter viruses. Representative images from plaque assays conducted on MDCK cells infected with the rA/Vic generated working stocks. Mock, rA/Vic-WT, and rA/Vic-NLuc images were captured after 5 days of incubation at 37°C and represent plaques formed by virus diluted at 10^{-4} . The mPlum plates were incubated for 8 days and the 10^{-2} dilution wells were imaged. These are representative images and the experiment was repeated twice.



*Plaques developed after 8 day incubation, compared to 5 day incubation of WT and NLuc viruses

Figure 21: Comparison of plaque areas formed by reporter and WT viruses. No significant differences between plaque areas (mm²) were observed between MDCK cells infected with either reporter virus compared to rA/Vic-WT. However, rA/Vic-mPlum plaque assay plates were incubated at 37°C for an additional three days than the rA/Vic-WT and rA/Vic-NLuc plates. Plaque assays with working stocks were repeated twice and plaques from representative wells were counted and used in the area analysis above.

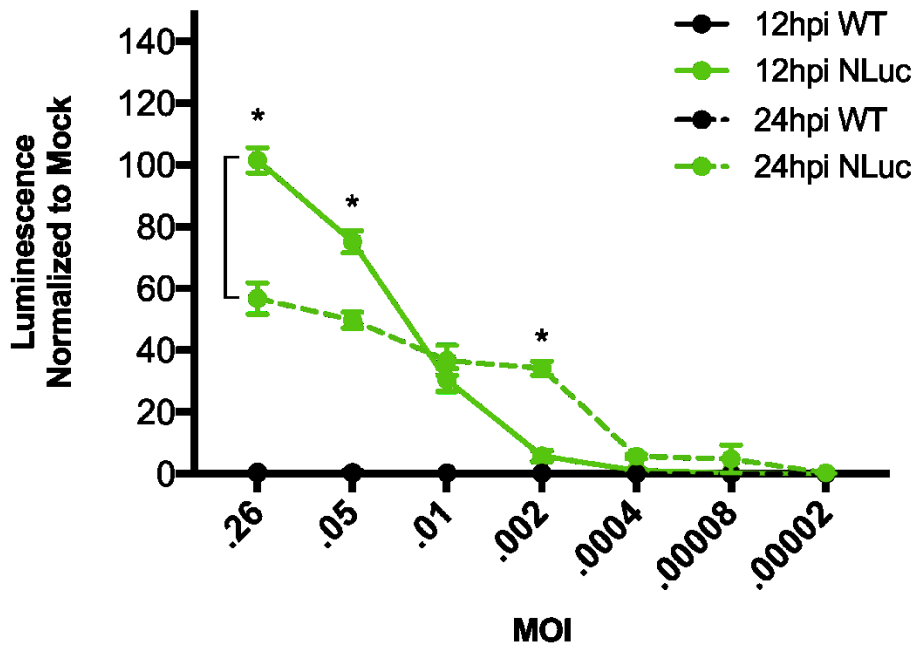


Figure 22: Luciferase activity of the rA/Vic-NLuc reporter virus. Luciferase activity of MDCK cells infected with rA/Vic-WT and rA/Vic-NLuc viruses as determined by Nano-Glo® Luciferase Assay. The assay was performed with five-fold dilutions of virus at 12 and 24 hpi and luminescence values were normalized to mock infected cells. The experiment was conducted twice with three replicate wells per sample. * denotes statistically significant differences between luciferase expression of rA/Vic-NLuc at 12 and 24hpi using a t test ($p < 0.05$).

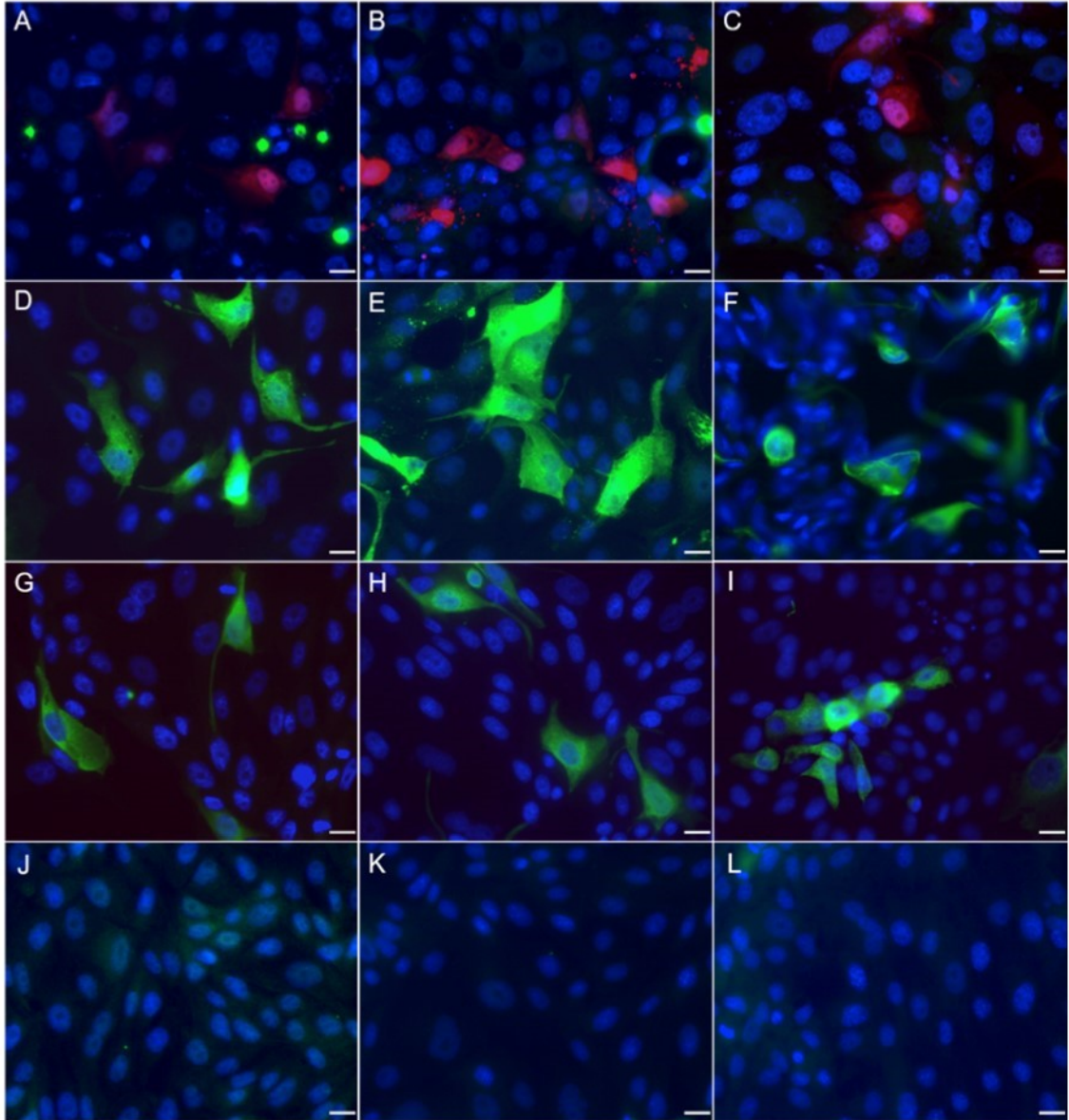


Figure 23: Fluorescence microscopy for evaluation of the rA/Vic-mPlum reporter virus. MDCK cells imaged (40x) at 12, 24, and 36 hours post transfection with pCAGGS-mPlum (A-C), and infection with rA/Vic-WT (D-F), rA/Vic-mPlum (G-I), and mock (J-L). Coverslips were stained for HA (green) and counterstained with DAPI for mounting. Cells are visibly infected with rA/Vic-mPlum (G-I), however no mPlum protein is detected (red). Images are representative of two replicates from a single experiment. Similar results were obtained in a repeat of the experiment.

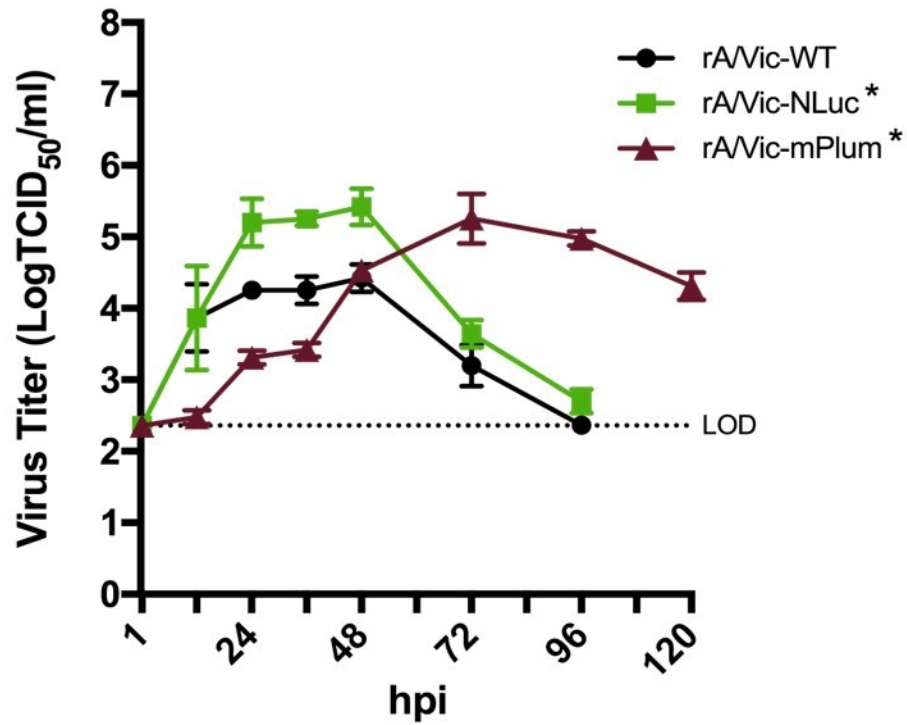


Figure 24: Replication kinetics of WT and reporter viruses. A low-multiplicity growth curve was performed in triplicate by infecting MDCK cells with an MOI of 0.001 of the generated recombinant rA/Vic viruses. TCID₅₀ plates for rA/Vic-WT and rA/Vic-NLuc were incubated for five days at 37°C, while the rA/Vic-mPlum plates were kept for an additional three days at 37°C before fixation and staining. Asterisks indicate a statistically significant difference of the overall growth curve compared to rA/Vic-WT using a two-way multiple-comparison ANOVA, $p < 0.01$. Graph shows mean \pm SD for two independent experiments with $n = 3$ per virus.

CHAPTER 5: REFERENCES

5.1 – Appendix

PA_GSG_2A gBlock including silent mutations (2,235bp)

GAAAGCAGGTACTGATTCAAAATGGAAGATTTTGTGCGACAATGCTTCAACCCGATGAT
TGTCGAACTTGCAGAAAAAGCAATGAAAGAGTATGGGGAGGATCTGAAAATTGAAACCA
ACAAATTTGCAGCAATATGCACTCACTTGGAGGTGTGTTTCATGTATTCAGATTTTCAT
TTCATCAATGAACAAGGCGAATCAATAGTGGTAGAACTTGACGATCCAAATGCACTGTT
AAAGCACAGATTTGAAATAATCGAGGGGAGAGACAGAACAATGGCCTGGACAGTAGTAA
ACAGTATCTGCAACACTACTGGAGCTGGAAAACCGAAGTTTCTACCGGATTTGTATGAT
TACAAAGAGAACAGATTCATCGAAATTGGAGTGACAAGGAGAGAAGTCCACATATATTA
CCTTGAAAAGGCCAATAAGATTAAATCTGAGAACACACACATTCACATTTTTTTCATTCA
CTGGGGAGGAAATGGCCACAAAGGCAGACTACACTCTCGACGAGGAAAGCAGGGCTAGG
ATTAATAACCAGGCTGTTTACCATAAGACAAGAAATGGCCAACAGAGGCCTCTGGGATTC
CTTTCGTCAGTCCGAAAGAGGCGAAGAAACAATTGAAGAAAAATTTGAAATCACAGGAA
CTATGCGTAGGCTTGCCGACCAAAGTCTCCACCGAACTTCTCCTGCCTTGAGAATTTT
AGAGCCTATGTGGATGGATTTCGAACCGAACGGCTGCATTGAGGGCAAGCTTTCTCAAAT
GTCCAAAGAAGTGAATGCCCAAATTGAACCTTTTCTGAAGACAACACCAAGACCAATCA
AACTTCCTAATGGACCTCCTTGTTATCAGAGGTCCAAATTCCTCCTGATGGATGCTTTA
AAATTGAGCATTGAAGACCCAAGTCACGAAGGAGAAGGGATCCCATTATATGATGCGAT
CAAGTGCATAAAAACATTCTTTGGATGGAAAGAACCTTATATAGTCAAACCACACGAAA
AGGGAATAAATTCAAATTACCTGCTGTTCATGGAAGCAAGTACTGTCAGAATTGCAGGAC
ATTGAAAATGAGGAGAAGATTCCAAGAACTAAAAACATGAAGAAAACGAGTCAACTGAA
GTGGGCTCTTGGTGAAAACATGGCACCAGAGAAGGTAGACTTTGAAAACCTGCAGAGACA
TAAGCGATTTGAAGCAATATGATAGTGACGAACCTGAATTAAGGTCACTTTCAAGCTGG
ATGCAGAGTGAGTTCAACAAGGCCTGTGAGCTAACTGATTTCAGTCTGGATAGAGCTCGA
TGAAATTGGAGAGGACGTAGCCCCAATTGAGCACATTGCAAGCATGAGAAGGAATTATT
TCACAGCAGAGGTGTCCCATTTGTAGAGCTACTGAATACATAATGAAGGGAGTATACATT
AACACTGCCCTGCTCAATGCATCCTGTGCAGCAATGGACGATTTTCAACTAATTCCCAT
GATAAGCAAGTGCAGAATAAGAGGGGAAGGCGAAAAACCAATTTATATGGATTTCATCA
TAAAGGGAAGATCTCATTTAAGGAATGACACAGACGTGGTAAATTTTGTGAGCATGGAG
TTTTCTCTCACAGACCCGAGACTTGAACCACATAAATGGGAGAAATACTGTGTCCTTGA
GATAGGAGATATGTTACTAAGAAGTGCCATAGGCCAAATTTCAAGACCGATGTTCTTGT
ATGTGAGGACAAACGGAACATCAAAGGTCAAAATGAAATGGGGAATGGAGATGAGACGT
TGCCTCCTTCAGTCACTCCAGCAGATCGAGAGCATGATTGAAGCCGAGTCCTCAGTTAA
AGAGAAAGACATGACCAAAGAGTTTTTTGAGAATAAATCAGAAGCATGGCCCATTTGGGG
AGTCCCCCAAGGGAGTGGAAGAAGGTTCCATTGGGAAAGTCTGTAGGACTCTATTGGCT
AAGTCAGTATTCAATAGCCTGTATGCATCACCACAATTGGAAGGATTTTCAGCGGAGTC
AAGAAAACCTGCTCCTTGTTGTTTCAGGCTCTTAGGGACAACCTCGAACCTGGGACCTTTG
ATCTTGGGGGGCTATATGAAGCAATTGAGGAGTGCCTGATTAATGATCCCTGGGTTCTT

TTGAACGCCTCCTGGTTTAATAGCTTTCTTACTCACGCCTTGAAAGGAAGCGGAGCCAC
GAACTTCTCTCTGTTAAAGCAAGCAGGAGACGTGGAAGAAAACCCCGGTCCC

NLuc-PAt50 gBlock with 3'UTR (621bp)

ATGGTCTTCACACTCGAAGATTTTCGTTGGGGACTGGCGACAGACAGCCGGCTACAACCT
GGACCAAGTCCTTGAACAGGGAGGTGTGTCCAGTTTGTTCAGAATCTCGGGGTGTCCG
TAACTCCGATCCAAAGGATTGTCCTGAGCGGTGAAAATGGGCTGAAGATCGACATCCAT
GTCATCATCCCGTATGAAGGTCTGAGCGGCGACCAAATGGGCCAGATCGAAAAAATTTT
TAAGGTGGTGTACCCTGTGGATGATCATCACTTTAAGGTGATCCTGCACTATGGCACAC
TGGTAATCGACGGGGTTACGCCGAACATGATCGACTATTTTCGGACGGCCGTATGAAGGC
ATCGCCGTGTTTCGACGGCAAAAAGATCACTGTAACAGGGACCCTGTGGAACGGCAACAA
AATTATCGACGAGCGCCTGATCAACCCCGACGGCTCCCTGCTGTTCCGAGTAACCATCA
ACGGAGTGACCGGCTGGCGGCTGTGCGAACGCATTCTGGCGTGCTCAATGCGTCTTGGT
TCAACTCCTTCTGACACATGCATTAAAATAGTTATGGCAGTGCTGCTATTTGTTATCC
GTACTGTCCAAAAAAGTACCTTGTTTCTACT

mPlum-PAt50 with 3'UTR (790bp)

ATGGTGAGCAAGGGCGAGGAGGTCATCAAGGAGTTCATGCGCTTCAAGGAGCACATGGA
GGGCTCCGTGAACGGCCACGAGTTCGAGATCGAGGGCGAGGGCGAGGGCCGCCCTACG
AGGGCACCCAGACCGCCAGGCTGAAGGTGACCAAGGGTGGCCCCCTGCCCTTCGCCTGG
GACATCCTGTCCCCTCAGATCATGTACGGCTCCAAGGCCTACGTGAAGCACCCCGCCGA
CATCCCCGACTACTTGAAGCTGTCCTTCCCCGAGGGCTTCAAGTGGGAGCGCGTGATGA
ACTTCGAGGACGGCGGCGTGGTGACCGTGACCCAGGACTCCTCCCTGCAGGACGGCGAG
TTCATCTACAAGGTGAAGGTGCGCGGCACCAACTTCCCCTCCGACGGCCCCGTAATGCA
GAAGAAGACCATGGGCTGGGAGGCCTCCTCCGAGCGGATGTACCCCGAGGACGGCGCCC
TGAAGGGCGAGATGAAGATGAGGCTGAGGCTGAAGGACGGCGGCCACTACGACGCCGAG
GTCAAGACCACCTACATGGCCAAGAAGCCCGTGCAGCTGCCCGGCGCCTACAAGACCGA
CATCAAGCTGGACATCACCTCCCACAACGAGGACTACACCATCGTGGAACAGTACGAGC
GCGCCGAGGGCCGCCACTCCACCGGCGCCTAAGTGCTCAATGCGTCTTGGTTCAACTCC
TTCCTGACACATGCATTAAAATAGTTATGGCAGTGCTGCTATTTGTTATCCGTA CTGTC
CAAAAAAGTACCTTGTTTCTACT

5.2 – Bibliography

- ¹ “Influenza (Flu).” Centers for Disease Control and Prevention, Centers for Disease Control and Prevention, 3 Oct. 2017, www.cdc.gov/flu/keyfacts.htm.
- ² Flint, S. Jane, et al. *Principles of Virology*. ASM Press, 2015. Page 392.
- ³ “Influenza (Flu).” Centers for Disease Control and Prevention, Centers for Disease Control and Prevention, 27 Sept. 2017, www.cdc.gov/flu/about/viruses/types.htm.
- ⁴ “Influenza (Flu).” Centers for Disease Control and Prevention, Centers for Disease Control and Prevention, 5 Oct. 2017, www.cdc.gov/flu/about/disease/spread.htm.
- ⁵ Bean, B. “Survival of Influenza Viruses on Environmental Surfaces.” *The Journal of Infectious Diseases*, vol. 146, no. 1, 1 July 1982, pp. 47–51.
- ⁶ Wu, Nai-Huei, et al. “The Differentiated Airway Epithelium Infected by Influenza Viruses Maintains the Barrier Function despite a Dramatic Loss of Ciliated Cells.” *Scientific Reports*, vol. 6, no. 1, 22 Dec. 2016, doi:10.1038/srep39668.
- ⁷ Biggerstaff, Matthew, et al. “Estimates of the Reproduction Number for Seasonal, Pandemic, and Zoonotic Influenza: a Systematic Review of the Literature.” *BMC Infectious Diseases*, vol. 14, no. 1, 4 Sept. 2014, doi:10.1186/1471-2334-14-480.
- ⁸ Plotkin, Stanley A., and Walter A. Orenstein. *Vaccines*. Saunders Elsevier, 2008.
- ⁹ Centers for Disease Control and Prevention (CDC): Estimates of deaths associated with seasonal influenza—United States, 1976-2007. *MMWR Morb Mortal Wkly Rep* 2010; 59: pp. 1057-1062
- ¹⁰ “Influenza (Seasonal).” World Health Organization, World Health Organization, www.who.int/mediacentre/factsheets/fs211/en/.
- ¹¹ Bouvier, Nicole M., and Peter Palese. “The Biology of Influenza Viruses.” *Vaccine*, vol. 26, 12 Sept. 2008, doi:10.1016/j.vaccine.2008.07.039.
- ¹² Breen, Michael, et al. “Replication-Competent Influenza A Viruses Expressing Reporter Genes.” *Viruses*, vol. 8, no. 7, 2016, p. 179., doi:10.3390/v8070179.

-
- ¹³ Wohlgemuth, Nicholas, et al. "The M2 Protein of Live, Attenuated Influenza Vaccine Encodes a Mutation That Reduces Replication in Human Nasal Epithelial Cells." *Vaccine*, vol. 35, no. 48, 2017, pp. 6691–6699., doi:10.1016/j.vaccine.2017.10.018.
- ¹⁴ Boivin, Stephane, et al. "Influenza A Virus Polymerase: Structural Insights into Replication and Host Adaptation Mechanisms." *Journal of Biological Chemistry*, vol. 285, no. 37, 2010, pp. 28411–28417., doi:10.1074/jbc.r110.117531.
- ¹⁵ Huang, Xiaofeng, et al. "An NS-Segment Exonic Splicing Enhancer Regulates Influenza A Virus Replication in Mammalian Cells." *Nature Communications*, vol. 8, 2017, p. 14751., doi:10.1038/ncomms14751.
- ¹⁶ Steinhauer, David A., et al. "Lack of Evidence for Proofreading Mechanisms Associated with an RNA Virus Polymerase." *Gene*, vol. 122, no. 2, 15 Dec. 1992, pp. 281–288., doi:10.1016/0378-1119(92)90216-c.
- ¹⁷ Boni, Maciej F. "Vaccination and Antigenic Drift in Influenza." *Vaccine*, vol. 26, 2008, doi:10.1016/j.vaccine.2008.04.011.
- ¹⁸ Matrosovich, M. N., et al. "Human and Avian Influenza Viruses Target Different Cell Types in Cultures of Human Airway Epithelium." *Proceedings of the National Academy of Sciences*, vol. 101, no. 13, 15 Mar. 2004, pp. 4620–4624., doi:10.1073/pnas.0308001101.
- ¹⁹ Murphy, Brian R., et al. "Association of Serum Anti-Neuraminidase Antibody with Resistance to Influenza in Man." *New England Journal of Medicine*, vol. 286, no. 25, 22 June 1972, pp. 1329–1332., doi:10.1056/nejm197206222862502.
- ²⁰ Krammer, Florian, et al. "NAction! How Can Neuraminidase-Based Immunity Contribute to Better Influenza Virus Vaccines?" *MBio*, vol. 9, no. 2, 3 Apr. 2018, doi:10.1128/mbio.02332-17.
- ²¹ Chen, Yao-Qing, et al. "Influenza Infection in Humans Induces Broadly Cross-Reactive and Protective Neuraminidase-Reactive Antibodies." *Cell*, vol. 173, no. 2, 5 Apr. 2018, doi:10.1016/j.cell.2018.03.030.
- ²² Parrish, Colin R., et al. "Influenza Virus Reservoirs and Intermediate Hosts: Dogs, Horses, and New Possibilities for Influenza Virus Exposure of Humans." *Journal of Virology*, vol. 89, no. 6, 24 Mar. 2014, pp. 2990–2994., doi:10.1128/jvi.03146-14.

-
- ²³ Sauer, Anne-Kathrin, et al. "Characterization of the Sialic Acid Binding Activity of Influenza A Viruses Using Soluble Variants of the H7 and H9 Hemagglutinins." *PLoS ONE*, vol. 9, no. 2, 21 Feb. 2014, doi:10.1371/journal.pone.0089529.
- ²⁴ Taubenberger, Jeffery K., and David M. Morens. "1918 Influenza: the Mother of All Pandemics." *Emerging Infectious Diseases*, vol. 12, no. 1, Jan. 2006, pp. 15–22., doi:10.3201/eid1209.050979.
- ²⁵ Kilbourne, Edwin D. "Influenza Pandemics of the 20th Century." *Emerging Infectious Diseases*, vol. 12, no. 1, 2006, pp. 9–14., doi:10.3201/eid1201.051254.
- ²⁶ Kuiken, T., et al. "Host Species Barriers to Influenza Virus Infections." *Science*, vol. 312, no. 5772, 2006, pp. 394–397., doi:10.1126/science.1122818.
- ²⁷ "Influenza Antiviral Drug Resistance." *Centers for Disease Control and Prevention*, Centers for Disease Control and Prevention, 10 Jan. 2018, www.cdc.gov/flu/about/qa/antiviralresistance.htm.
- ²⁸ Weir, Jerry P., and Marion F. Gruber. "An Overview of the Regulation of Influenza Vaccines in the United States." *Influenza and Other Respiratory Viruses*, vol. 10, no. 5, 2016, pp. 354–360., doi:10.1111/irv.12383.
- ²⁹ Minor, Philip D. "Vaccines against Seasonal and Pandemic Influenza and the Implications of Changes in Substrates for Virus Production." *Clinical Infectious Diseases*, vol. 50, no. 4, 15 Feb. 2010, pp. 560–565., doi:10.1086/650171.
- ³⁰ Lu, B., et al. "Improvement of Influenza A/Fujian/411/02 (H3N2) Virus Growth in Embryonated Chicken Eggs by Balancing the Hemagglutinin and Neuraminidase Activities, Using Reverse Genetics." *Journal of Virology*, vol. 79, no. 11, 12 June 2005, pp. 6763–6771., doi:10.1128/jvi.79.11.6763-6771.2005.
- ³¹ Russell, Kevin L., et al. "Effectiveness of the 2003–2004 Influenza Vaccine among U.S. Military Basic Trainees: a Year of Suboptimal Match between Vaccine and Circulating Strain." *Vaccine*, vol. 23, no. 16, 2005, pp. 1981–1985., doi:10.1016/j.vaccine.2004.10.023.
- ³² Samji, Tasleem. "Influenza A: Understanding the Viral Life Cycle." *Influenza A: Understanding the Viral Life Cycle*, Dec. 2009, www.ncbi.nlm.nih.gov/pmc/articles/PMC2794490/.

-
- ³³ Wu, Winco Wh, et al. "Nuclear Import of Influenza A Viral Ribonucleoprotein Complexes Is Mediated by Two Nuclear Localization Sequences on Viral Nucleoprotein." *Virology Journal*, vol. 4, no. 1, 4 June 2007, p. 49., doi:10.1186/1743-422x-4-49.
- ³⁴ Li, Sai, et al. "PH-Controlled Two-Step Uncoating of Influenza Virus." *Biophysical Journal*, vol. 106, no. 7, 2014, pp. 1447–1456., doi:10.1016/j.bpj.2014.02.018.
- ³⁵ Resa-Infante, Patricia, et al. "The Influenza Virus RNA Synthesis Machine." *RNA Biology*, vol. 8, no. 2, 1 Mar. 2011, pp. 207–215., doi:10.4161/rna.8.2.14513.
- ³⁶ Neumann, G., et al. "Orthomyxovirus Replication, Transcription, and Polyadenylation." *SpringerLink*, Springer, Berlin, Heidelberg, 1 Jan. 1970, link.springer.com/chapter/10.1007/978-3-662-06099-5_4.
- ³⁷ Kawaguchi, Atsushi, and Kyosuke Nagata. "De Novo Replication of the Influenza Virus RNA Genome Is Regulated by DNA Replicative Helicase, MCM." *The EMBO Journal*, vol. 26, no. 21, 11 Oct. 2007, pp. 4566–4575., doi:10.1038/sj.emboj.7601881.
- ³⁸ Kawaguchi, A., et al. "Involvement of Influenza Virus PA Subunit in Assembly of Functional RNA Polymerase Complexes." *Journal of Virology*, vol. 79, no. 2, 20 Jan. 2004, pp. 732–744., doi:10.1128/jvi.79.2.732-744.2005.
- ³⁹ Xing, W., Barauskas, O., Kirschberg, T., Niedziela-Majka, A., Clarke, M., Birkus, G., & ... Feng, J. Y. (2017). Biochemical characterization of recombinant influenza A polymerase heterotrimer complex: Endonuclease activity and evaluation of inhibitors. *Plos ONE*, 12(8), 1-14. doi:10.1371/journal.pone.0181969
- ⁴⁰ Vreede, Frank T., and Ervin Fodor. "The Role of the Influenza Virus RNA Polymerase in Host Shut-Off." *Virulence*, vol. 1, no. 5, 2010, pp. 436–439., doi:10.4161/viru.1.5.12967.
- ⁴¹ Samji, Tasleem. "Influenza A: Understanding the Viral Life Cycle." *Influenza A: Understanding the Viral Life Cycle*, Dec. 2009, www.ncbi.nlm.nih.gov/pmc/articles/PMC2794490/.
- ⁴² Mattia, Kimberly, et al. "Dengue Reporter Virus Particles for Measuring Neutralizing Antibodies against Each of the Four Dengue Serotypes." *PLoS ONE*, vol. 6, no. 11, 2011, doi:10.1371/journal.pone.0027252.

-
- ⁴³ Schoggins, J. W., et al. “Dengue Reporter Viruses Reveal Viral Dynamics in Interferon Receptor-Deficient Mice and Sensitivity to Interferon Effectors in Vitro.” *Proceedings of the National Academy of Sciences*, vol. 109, no. 36, 2012, pp. 14610–14615., doi:10.1073/pnas.1212379109.
- ⁴⁴ Freeman, M. C., et al. “Coronavirus Replicase-Reporter Fusions Provide Quantitative Analysis of Replication and Replication Complex Formation.” *Journal of Virology*, vol. 88, no. 10, 2014, pp. 5319–5327., doi:10.1128/jvi.00021-14.
- ⁴⁵ Singh, Brajesh K., et al. “Cell-to-Cell Contact and Nectin-4 Govern Spread of Measles Virus from Primary Human Myeloid Cells to Primary Human Airway Epithelial Cells.” *Journal of Virology*, vol. 90, no. 15, 2016, pp. 6808–6817., doi:10.1128/jvi.00266-16.
- ⁴⁶ Breen, Michael, et al. “Replication-Competent Influenza A Viruses Expressing Reporter Genes.” *Viruses*, vol. 8, no. 7, 2016, p. 179., doi:10.3390/v8070179.
- ⁴⁷ Shinya, K., et al. “Characterization of a Neuraminidase-Deficient Influenza A Virus as a Potential Gene Delivery Vector and a Live Vaccine.” *Journal of Virology*, vol. 78, no. 6, 2004, pp. 3083–3088., doi:10.1128/jvi.78.6.3083-3088.2004.
- ⁴⁸ Kittel, Christian, et al. “Rescue of Influenza Virus Expressing GFP from the NS1 Reading Frame.” *Virology*, vol. 324, no. 1, 2004, pp. 67–73., doi:10.1016/j.virol.2004.03.035.
- ⁴⁹ Pan, Weiqi, et al. “Visualizing Influenza Virus Infection in Living Mice.” *Nature Communications*, vol. 4, 2013, doi:10.1038/ncomms3369.
- ⁵⁰ Manicassamy, B., et al. “Analysis of in Vivo Dynamics of Influenza Virus Infection in Mice Using a GFP Reporter Virus.” *Proceedings of the National Academy of Sciences*, vol. 107, no. 25, 2010, pp. 11531–11536., doi:10.1073/pnas.0914994107.
- ⁵¹ Fukuyama, Satoshi, et al. “Multi-Spectral Fluorescent Reporter Influenza Viruses (Color-Flu) as Powerful Tools for in Vivo Studies.” *Nature Communications*, vol. 6, no. 1, 25 Mar. 2015, doi:10.1038/ncomms7600.
- ⁵² Tran, V., et al. “Highly Sensitive Real-Time In Vivo Imaging of an Influenza Reporter Virus Reveals Dynamics of Replication and Spread.” *Journal of Virology*, vol. 87, no. 24, 2013, pp. 13321–13329., doi:10.1128/jvi.02381-13.

-
- ⁵³ “MPlum Fluorescent Protein.” Clontech,
www.clontech.com/US/Products/Fluorescent_Proteins_and_Reporters/Fluorescent_Proteins_by_Name/mPlum_Fluorescent_Protein.
- ⁵⁴ Day, Richard N., and Michael W. Davidson. “The Fluorescent Protein Palette: Tools for Cellular Imaging.” *Chemical Society Reviews*, vol. 38, no. 10, 2009, p. 2887., doi:10.1039/b901966a.
- ⁵⁵ Shcherbo, Dmitry, et al. “Far-Red Fluorescent Tags for Protein Imaging in Living Tissues.” *Biochemical Journal*, vol. 418, no. 3, 2009, pp. 567–574., doi:10.1042/bj20081949.
- ⁵⁶ Hall, Mary P., et al. “Engineered Luciferase Reporter from a Deep Sea Shrimp Utilizing a Novel Imidazopyrazinone Substrate.” *ACS Chemical Biology*, vol. 7, no. 11, 2012, pp. 1848–1857., doi:10.1021/cb3002478.
- ⁵⁷ Hitoshi, Niwa, et al. “Efficient Selection for High-Expression Transfectants with a Novel Eukaryotic Vector.” *Gene*, vol. 108, no. 2, 1991, pp. 193–199., doi:10.1016/0378-1119(91)90434-d.
- ⁵⁸ “Influenza Viruses A, B.” *Virus Taxonomy: Classification and Nomenclature of Viruses: Sixth Report of the International Committee on the Taxonomy of Viruses*, by C. M. Fauquet, Springer-Verlag, 2012, pp. 296–298.
- ⁵⁹ Neumann, G., et al. “Generation of Influenza A Viruses Entirely from Cloned cDNAs.” *Proceedings of the National Academy of Sciences*, vol. 96, no. 16, 1999, pp. 9345–9350., doi:10.1073/pnas.96.16.9345.
- ⁶⁰ Peretz, Jackye, et al. “Estrogenic Compounds Reduce Influenza A Virus Replication in Primary Human Nasal Epithelial Cells Derived from Female, but Not Male, Donors.” *American Journal of Physiology-Lung Cellular and Molecular Physiology*, vol. 310, no. 5, 2016, doi:10.1152/ajplung.00398.2015.
- ⁶¹ Goto, Hideo, et al. “Mutations Affecting the Sensitivity of the Influenza Virus Neuraminidase to 4-Guanidino-2,4-Dideoxy-2,3-Dehydro-N-Acetylneuraminic Acid.” *Virology*, vol. 238, no. 2, 1997, pp. 265–272., doi:10.1006/viro.1997.8810.
- ⁶² Reed, L.j., and H. Muench. “A Simple Method Of Estimating Fifty Per Cent Endpoints12.” *American Journal of Epidemiology*, vol. 27, no. 3, 1938, pp. 493–497., doi:10.1093/oxfordjournals.aje.a118408.
- ⁶³ “Far Red Fluorescent Protein Vectors.” *Fluorescent Proteins by Color*, Takara Bio Company, 2018,
www.clontech.com/US/Support/Applications/Fluorescent_Proteins_by_Color/Far_Red.

-
- ⁶⁴ Spronken, Monique I., et al. "Optimisations and Challenges Involved in the Creation of Various Bioluminescent and Fluorescent Influenza A Virus Strains for In Vitro and In Vivo Applications." *Plos One*, vol. 10, no. 8, 4 Aug. 2015, doi:10.1371/journal.pone.0133888.
- ⁶⁵ Kumar, Amrita, et al. "Influenza Virus Exploits Tunneling Nanotubes for Cell-to-Cell Spread." *Scientific Reports*, vol. 7, 6 Jan. 2017, p. 40360., doi:10.1038/srep40360.
- ⁶⁶ Karlsson, Erik A., et al. "Visualizing Real-Time Influenza Virus Infection, Transmission and Protection in Ferrets." *Nature Communications*, vol. 6, no. 1, 6 Mar. 2015, doi:10.1038/ncomms7378.
- ⁶⁷ Truelove, Shaun, et al. "A Comparison of Hemagglutination Inhibition and Neutralization Assays for Characterizing Immunity to Seasonal Influenza A." *Influenza and Other Respiratory Viruses*, vol. 10, no. 6, 27 Nov. 2016, pp. 518–524., doi:10.1111/irv.12408.
- ⁶⁸ Wood, John M., et al. "Reproducibility of Serology Assays for Pandemic Influenza H1N1: Collaborative Study to Evaluate a Candidate WHO International Standard." *Vaccine*, vol. 30, no. 2, 5 Jan. 2012, pp. 210–217., doi:10.1016/j.vaccine.2011.11.019.
- ⁶⁹ Stephenson, Iain, et al. "Comparison of Neutralising Antibody Assays for Detection of Antibody to Influenza A/H3N2 Viruses: An International Collaborative Study." *Vaccine*, vol. 25, no. 20, 16 May 2007, pp. 4056–4063., doi:10.1016/j.vaccine.2007.02.039.
- ⁷⁰ Trombetta, Claudia, et al. "Overview of Serological Techniques for Influenza Vaccine Evaluation: Past, Present and Future." *Vaccines*, vol. 2, no. 4, 13 Oct. 2014, pp. 707–734., doi:10.3390/vaccines2040707.
- ⁷¹ Horimoto, Taisuke, and Yoshihiro Kawaoka. "Influenza: Lessons from Past Pandemics, Warnings from Current Incidents." *Nature Reviews Microbiology*, vol. 3, no. 8, 2005, pp. 591–600., doi:10.1038/nrmicro1208.
- ⁷² Murakami, Katsuhiko. "Faculty of 1000 Evaluation for Structural Basis of an Essential Interaction between Influenza Polymerase and Pol II CTD." F1000 - Post-Publication Peer Review of the Biomedical Literature, 2016, doi:10.3410/f.727132392.793526762.
- ⁷³ Neumann, G., et al. "Generation of Influenza A Viruses Entirely from Cloned CDNAs." *Proceedings of the National Academy of Sciences*, vol. 96, no. 16, 3 Aug. 1999, pp. 9345–9350., doi:10.1073/pnas.96.16.9345.

⁷⁴ Dong, Yangchao, et al. “Isolation of Endogenously Assembled RNA-Protein Complexes Using Affinity Purification Based on Streptavidin Aptamer S1.” *International Journal of Molecular Sciences*, vol. 16, no. 9, 16 Sept. 2015, pp. 22456–22472., doi:10.3390/ijms160922456.

5.3 – Curriculum Vitae

EMILY THOMPSON

thompsonemily@comcast.net
(303) 883-0722

EDUCATION

Johns Hopkins University Bloomberg School of Public Health

Aug. 2016 – Present

Sc.M., Molecular Microbiology and Immunology

Anticipated Graduation: May 2018

GPA 3.94

University of Denver

Sep. 2010 – June 2014

B.S. Molecular Biology, Graduation with Distinction

B.A. International Studies, Specialization in International Organizations & Security

Minors: Mathematics, Chemistry, and French

GPA 3.75, *Cum Laude*

CERTIFICATIONS

Vaccine Science and Policy Certificate

Johns Hopkins University Bloomberg School of Public Health, 2018

- Identified and critiqued cutting-edge strategies for vaccine development
- Analyzed Yellow Fever vaccine policy in Brazil and created recommendation statement
- Engaged with key stakeholders involved in formulating vaccine policy in the US

Public Health Emergency Preparedness Certificate

Johns Hopkins University Bloomberg School of Public Health, 2018

- Analyzed crisis risk communication techniques and prepared press release statements
- Researched and presented policy recommendations to the Maryland General Assembly

TECHNICAL SKILLS

Statistics: Stata, R

Data Visualization: ArcGIS, GraphPad Prism, Microsoft Office Suite

Languages: Advanced French– conversational, reading, and writing

Completed Honors Program at the Institutes for American Universities // Aix-en-Provence, France

PUBLIC HEALTH EXPERIENCE

Johns Hopkins Bloomberg School of Public Health // Dept. of Population, Family, and Reproductive Health

Research Assistant – Text4Father

May 2017 – Present

- Conducts research for systematic review of NIH-funded fatherhood study
- Assists with evidence-based mHealth program to engage fathers during pregnancy and early infancy

International Vaccine Access Center

Oct. 2016 – Jun. 2017

Data Abstractor

- Abstracted data for a systematic review to evaluate PCV effectiveness worldwide
- Contributed to PCV Product Assessment to provide the Gavi Secretariat with a synthesis of performance, effectiveness, and impact for current PCV products

Integrated Food Safety Center of Excellence

Jun. – Oct. 2014

Epidemiology Intern

- Composed summaries of WHO and CDC foodborne disease outbreak data
- Streamlined private wiki page for Colorado state epidemiologists

Office of U.S. Senator Michael Bennet

Aug. 2013 – May 2014

Intern to Senior Business Advisor and State Scheduler

- Created weekly reports for Senator Bennet regarding current issues of constituent concern
- Developed presentations on emerging technologies for state-wide business meetings

LABORATORY RESEARCH EXPERIENCE

Johns Hopkins Bloomberg School of Public Health // Department of Molecular Microbiology & Immunology

Andrew Pekosz Laboratory

Oct. 2016 – Present

- Creating a fluorescent influenza A reporter virus to allow real-time visualization of influenza infection

University of Colorado Anschutz // Department of Surgery

Jan. – Aug. 2016

Jonathan Roach Laboratory – *Characterization of Bile Acid Transporters in Biliary Atresia*

- Piloted experiments to evaluate immunological processes of pediatric liver disease

Greffex, Inc.

Oct. 2014 – Oct. 2015

Research Associate

- Influenced technical and analytical development of rapid-to-market vaccines
- Implemented practice and document standard in compliance with FDA protocols

National Jewish Health // Department of Allergy and Clinical Immunology

Rafeul Alam Laboratory – *Evaluating Immunological Profiles in Persistent Asthma*

-
- Characterized immunological mechanisms that drive asthma following exposure to various environmental factors

LEADERSHIP AND SERVICE

Johns Hopkins University // Undergraduate Public Health Studies Aug.– Dec. 2017
Teaching Assistant

- Led weekly laboratory session to reinforce key public health concepts including US healthcare infrastructure, epidemiology, biostatistics, and environmental health

Project C.U.R.E. // Department of Operations Sep. – Nov. 2014
Volunteer

- Supported shipment organization of medical equipment to Liberia during the 2014 Ebola epidemic
- Modernized biomedical equipment manual database documents sent to international aid recipients

University of Denver Model United Nations Feb. 2011 – Jun. 2013
Founder and President

- Negotiated logistical and financial support from the University Honors Program
- Established a strong organizational basis and grew membership to 200 members in three years
- Organized and hosted two annual conferences for over 250 high school students

International Model United Nations Association Apr. 2010 – Mar. 2012
Director, Security Council

- Authored documents on security issues in Pakistan, Kashmir, Yemen, and Chechnya
- Educated high school students on the structure and function of international organizations
- Moderated debate sessions at the National High School Model United Nations Conference

PATENTS AND PRESENTATIONS

Staerz, U., **Thompson, E.**, et al. Enhancement of Production of Adenoviral-based Gene Transfer Vectors. U.S. Patent Application 62/282,220, Patent Pending.

Crisis in Yemen – Debating Current World Events

University of Denver Spring Symposium // Denver, CO – May 7, 2011
Korbel School of International Studies

Exploring Asthma: TLR Ligands in IL-33 and ST2 Expression

University of Denver Honors Thesis Defense // Denver, CO – May 2, 2014

Generating an Influenza A Reporter Virus

Johns Hopkins University
Molecular Microbiology & Immunology Department Forum // Baltimore, MD

AWARDS AND FELLOWSHIPS

- **University of Denver Chancellor Scholar, 2010-2014**
- **Mortar Board Society, 2013-2014**
- **University of Denver Honors Program, 2010-2014**
- **Dean's List, 2010-2014**
- **Delta Omega Honor Society Nominee, 2018**